

MONOLITHIC INTEGRATION OF GLASS-BASED OPTICAL  
DEVICES VIA SOLUTION DOPING OF  
ERBIUM RARE-EARTH MATERIAL

KOW SIEW TING @ KOH SIEW TING

FACULTY OF SCIENCE  
UNIVERSITI MALAYA  
2009

MONOLITHIC INTEGRATION OF GLASS-BASED OPTICAL  
DEVICES VIA SOLUTION DOPING OF  
ERBIUM RARE-EARTH MATERIAL

KOW SIEW TING @ KOH SIEW TING

Dissertation submitted in Fulfillment  
Of the requirements  
For the master of Technology (Material Science)

Physic Department  
Faculty Science  
University Malaya  
Kuala Lumpur  
July 2009

UNIVERSITY OF MALAYA

ORIGINAL LITERARY WORK DECLARATION

Name of candidate : Kow Siew Ting @ Koh Siew Ting

IC/Password : 841110-05-5392

Registration/Matrix No: SGG070003

Name of Degree : Master of Technology (Material Science)

Title of dissertation : Monolithic Integration Of glass-based via solution doping of Erbium Rare-Earth material

Field of study:

I do solemnly and sincerely declare that:

1. I am the sole author/writer of this work;
2. This work is original;
3. Any use of any work in which copyright exists was done by way of fair dealing and for permitted purposes and any excerpt or extract from, or reference to or reproduction of any copyright work has been disclosed expressly and sufficiently and the title of the work and its authorship have been acknowledged in this work;
4. I do not have any actual knowledge nor I do ought reasonably to know that the making of this work constitute an infringement of any copyright work;
5. I hereby assign all and every rights in the copyright to this work to the University of Malaya ("UM"), who henceforth shall be owner of the copyright in this works and that any reproduction or use in any form or by any means whatever is prohibited without the written consent of UM having been first had and obtained;
6. I am fully aware that if in the course of making this work I have infringed any copyright whether intentionally or otherwise, I may be subject to legal action or any other action as may be determined by UM.

---

Candidate's Signature

Date: 20.07.2009

Subscribed and solemnly declared before,

---

Witness's Signature

Date: 20.07.2009

Name: Prof. Harith Bin Ahmad

Designation: Professor

## ABSTRACT

This thesis describes novel experimental methods in solution doping based on dipping (non-selective area) and dripping via a syringe/pipette (selective area doping). Silica soot layers deposited via Flame Hydrolysis Deposition were pre-sintered prior to solution doping. The doped pre-sintered soot was then consolidated to form dense silica layers. The variations in the number of pores, layer thickness, and dopant (erbium) concentration play major roles in the quality of the resulting glass layer.

Optimisation and subsequent characterisation of the pre-sintered layers in terms of surface morphology and structure were carried out. It was found that samples pre-sintered at 850°C were optimal, allowing solution doping to be performed. Saturation of the dipping period was achieved within 20 minutes following immersion of the sample into an erbium-trichloride in de-ionised water solution.

In selective area doping, both single and multi-cycle dripping approaches were adopted. Erbium ion concentration increased as the number of droplets increases. Ring effects were also observed at high droplet counts.

## ABSTRAK

Disertasi ini menceritakan tentang pendopan dengan menggunakan larutan akueus secara celupan dinamakan pendopan secara keseluruhan dan titisan dengan pipet atau penyuntik dinamakan pendopan pada kawasan terpilih lapisan. Lapisan “soot” silika diendapkan dengan menggunakan pengendapan secara hidrolisis api diikuti pendopan dengan larutan akueus dalam lapisan “soot” silika. Dalam proses pendopan secara keseluruhan, kelarutan ion erbiium dalam lapisan “soot” silika diubah dengan suhu sinter separa yang berbeza, kepekatan larutan dan masa celupan. Untuk proses pendopan pada kawasan terpilih, diameter bulatan, ketebalan cincin dan kelarutan atau penyebaran ion erbiium dalam lapisan “soot” silika telah dikaji dengan menggunakan cara menitik yang berbeza dan suhu substrat yang lain.

Morfologi dan struktur dalam lapisan “soot” silika dikaji dengan menggunakan mikroskop elektron imbasan pancaran medan (FESEM). Morfologi sampel berubah mengikuti suhu sinter separa yang berbeza. Struktur lapisan “soot” silika menjadi kuat apabila suhu sinter separa yang tinggi. Saiz zarah menjadi besar disebabkan kesan “jerutan”. Dalam graf saiz liang menunjukkan bilangan liang adalah terbanyak dalam suhu sinter separa 850°C. Ketebalan lapisan silika menjadi nipis apabila suhu sinter separa menaik. Ketebalan lapisan juga menjadi lebih nipis setelah dicelup dalam larutan akueus. Ketelaruatan ion erbiium bertambah apabila kepekatan larutan bertambah. Dalam kajian masa celupan, 20 minit menunjukkan masa ketepuan untuk keterlarutan ion erbiium dalam sampel semasa mencelup dalam larutan akueus.

Dalam kajian pendopan secara kawasan terpilih, kami menggunakan dua cara untuk menyuntik larutan akueus dalam lapisan silika iaitu secara terusan dan berbilang kali. Ketelaruatan ion erbiium dalam lapisan silika bertambah apabila bilangan titik yang disuntik bertambah. Di samping itu, ketelaruatan ion erbiium juga bertambah mengikuti kawasan bulatan iaitu pusat, tengah dan cincin. Di antara ketiga-tiga kawasan, kawasan cincin adalah ketelaruatan ion erbiium yang tertinggi. Diameter cincin juga bertambah dengan isipadu setiap titik dan bilangan titik yang disuntik.

## **ACKNOWLEDGEMENT**

I would like to express my deepest gratitude to my supervisor, Professor Harith Ahamd and co-supervisor Dr. Faisal Rafiq Mahamd Adikan for their useful advices and encouragements throughout the period of this dissertation. My gratitude extends to several members of Photonics Laboratory, such as Chong Wu Yi, Pua Chang Hong, Alvin Law Wen Pin, Lim Weng Hong, Sua Yong Meng and Yap Yen for their helpful suggestions and technical assistance. I would like to express my sincere thanks to my parents and some of my friends that always supporting me in completing this work. Last but no least, I would like to express my grateful acknowledgement to Universiti of Malaya for providing me this opportunity to carry out this dissertation. This experience will definitely benefits my future life.

## TABLE OF CONTENTS

	<b>Pages</b>
<b>Abstract</b>	<b>ii</b>
<b>Abstrack</b>	<b>iii</b>
<b>Acknowledgement</b>	<b>iv</b>
<b>Table of contents</b>	<b>v</b>
<b>List of figures</b>	<b>viii</b>
<b>List of tables</b>	<b>xi</b>
<b>Abbreviation</b>	<b>xii</b>

## CHAPTER 1 INTRODUCTION

1.1 Optical telecommunication	1
1.2 Integrated optics	2
1.3 Optical amplifiers	3
1.4 Aim of research/Objectives	4
1.5 Outline of thesis	5
Reference	6

## CHAPTER 2 THEORY AND FABRICATION OF SILICA LAYER

2.1 Silica-on-silicon technology for integrated optics	7
2.2 Doped glass structure and properties	8
2.3 Glass host composition	10
2.4 Principle of optical amplifier	12
2.5 Amplifier properties and parameters	14
2.6 Method for fabrication silica soot layer	15
2.6.1 Flame Hydrolysis Deposition (FHD)	15
2.6.2 Plasma Enhanced Chemical Vapour Deposition (PECVD)	18
2.6.3 Sol-gel	19
2.7 Review of solution doping	21
2.8 Summary	23
Reference	23

## **CHAPTER 3 SOLUTION DOPING**

3.1 Introduction to rare-earth doping techniques	25
3.2 Principle of solution doping	26
3.3 Experimental method	26
3.4 Principle of Pre-sintering in soot layer	28
3.5 Pre-sintering soot layer	29
3.6 Non-selective area doping	36
3.7 Summary	43
References	43

## **CHAPTER 4 SELECTIVE AREA DOPING**

4.1 Introduction	45
4.2 Review of selective area doping	45
4.3 Selective area set up (experimental method )	46
4.4 Selective area by syringe	48
4.4.1 Diameter of selective area doping area	48
4.4.2 Erbium ion concentration Vs number of droplets	54
4.4.3 Distribution of erbium ion concentration	57
4.5 Selective area by pipette & hotplate	60
4.5.1 Diameter of selective area doping area	61
4.5.2 Erbium ion concentration Vs number of droplets	67
4.5.3 Distribution of erbium ion concentration	68
4.6 Summary	69
References	70

## **CHAPTER 5**

5.1 Summary	71
5.2 Conclusion	72
5.3 Future works	73
References	74





## List of figure

<b>Chapter 2</b>	<b>Pages</b>
2.1 Three types of planar waveguide (a) rib (b) ridge, and (c) buried	8
2.2 (a) schematic of three-dimensional tetrahedral arrangement in fused silica glass. (b) a diagram of two-dimensional matrix of silicon and oxygen atoms.	9
2.3 A schematic showing the silica glass matrix disrupted by the addition of modifier ions	10
2.4 Energy level diagram of a free $\text{Er}^{3+}$ ion.	13
2.5 Schematic and photo of deposition step of FHD. The soot is then consolidated to form a glassy layer.	16
2.6 Schematic of burner's position and turntable rotate in flame hydrolysis deposition.	17
2.7 PECVD deposition chamber and process schematic.	19
2.8 Diagram of the sol-gel synthesis route.	21
<b>Chapter 3</b>	
3.1 Necking of particles during pre-sintering process	29
3.2 FESEM images: The morphology and microstructure of silica soot layers at different pre-sintering temperatures before solution doping with magnification 30k x. (a) 750°C (b) 800°C (c) 850°C (d) 900°C (e) 950°C	31
3.3 FESEM images: The morphology and microstructure of silica soot layer at different pre-sintering temperatures after 0.1M erbium chloride ( $\text{ErCl}_3 \cdot 6\text{H}_2\text{O}$ ) aqueous solution doping with magnification 30kx. (a) 750°C (b) 800°C (c) 850°C (d) 900°C (e) 950°C	32
3.4 A diagram showing the indication of beam area injection by EDX for silica soot layer pre-sintered at 950°C after solution doping.	33
3.5 Graph for number of pores in silica porous soot layer in different pre-sintering temperature.	34
3.6 Graph shows that the thickness of soot layers varies in different temperature.	35
3.7 The pictures of 0.1M erbium chloride doped samples in different pre-sintering temperature and consolidated in 1320°C.	37
3.8 Erbium concentration, at% in varied different pre-sintering temperature in 0.1M erbium chloride ( $\text{ErCl}_3 \cdot 6\text{H}_2\text{O}$ ) before and after consolidation in 1320°C.	38
3.9 Variation of $\text{Er}^{3+}$ concentration with change in molarity of solution	

ErCl <sub>3</sub> .6H <sub>2</sub> O aqueous.	39
3.10 Images show the changes in molarity of erbium chloride (ErCl <sub>3</sub> .6H <sub>2</sub> O) solution doping in silica layer after consolidation 1320°C. (a) 0.02M (b) 0.04M (c) 0.06M (d) 0.08M (e) 0.1M	40
3.11. Refractive index of Erbium doped silica layer as a function of molarity of solution	41
3.12. Concentration ion Er <sup>3+</sup> incorporated dependence dipping duration.	42
<b>Chapter 4</b>	
4.1 Selective area doping using a syringe (number indicating number of droplets applied).	47
4.2 Pictures of selective area doped with 0.1M erbium chloride (ErCl <sub>3</sub> .6H <sub>2</sub> O) in pre-sintering temperature 850°C of silica soot layer by using syringe (a) one cycle (b) multiple cycles	50
4.3 Pictures of failed samples in selective area doped with 0.1M erbium chloride (ErCl <sub>3</sub> .6H <sub>2</sub> O) in pre-sintering temperature 850°C of silica soot layer by using syringe (a) one cycle (b) multiple cycles	50
4.4 Graph of diameter of circle, mm in change of droplets doped with 0.1M erbium chloride (ErCl <sub>3</sub> .6H <sub>2</sub> O) by using syringe (one cycle)	52
4.5 Graph showed that ring's width, mm in change of droplets with 0.1M erbium chloride (ErCl <sub>3</sub> .6H <sub>2</sub> O) by using syringe (one cycle)	52
4.6. Graph showed that diameter of circle, mm in change of droplets with 0.1M erbium chloride (ErCl <sub>3</sub> .6H <sub>2</sub> O) by using syringe (multiple cycles)	53
4.7. Graph showed that ring's width, mm in change of droplets with 0.1M erbium chloride (ErCl <sub>3</sub> .6H <sub>2</sub> O) by using syringe (multiple cycles)	53
4.8 Position of circle in selective area doping measured by EDX	55
4.9. Graph showing different position of erbium concentration, wt% with change in number of droplets in 0.1M erbium chloride by using syringe (one cycle)	56
4.10. Graph showing different position of erbium concentration, wt% with change in number of droplets in 0.1M erbium chloride by using syringe (multiple cycles)	56
4.11. EDX profile across circle in selective area doping in 0.1M erbium chloride by using syringe (one cycle) (a) 3 droplets (b) 9 droplets	58
4.12. EDX profile across circle in selective area doping in 0.1M erbium chloride by using syringe (multiple cycles) (a) 3 droplets (b) 9 droplets	59
4.13 Schematic of selective area doping by using pipette and hotplate to adjust the temperature.	61

4.14	Pictures of samples in selective area doping by using pipette (a) volume of droplets varied from 0.1 $\mu$ to 1.3 $\mu$ L drip in 0.02M erbium chloride (b) multiple cycles with change in number of droplets drip in 0.02M erbium chloride (c) hotplate and 0.5 $\mu$ L volume of droplets drip in 0.1M erbium chloride	62
4.15	Graph showing the diameter of circle, mm varied with volume of erbium chloride, $\mu$ L.	63
4.16	Graph showing the diameter of circle, mm varied with number of droplets in multiple cycles	65
4.17	Graph showing ring width, mm varied with number of droplets in multiple cycles	65
4.18	Graph showing diameter of circle, mm varied with temperature, $^{\circ}$ C by using hotplate and pipette.	66
4.19	Graph showing erbium ion concentration, wt% with change in number of droplets in ring position dope with 0.02M erbium chloride by using pipette (multiple cycles)	68
4.20	Images showing the position of circle during line scan was taken by using EDX.	69
4.21	EDX profile across circle in selective area doping in 0.1M erbium chloride by using pipette for 50 droplets. (multiple cycles)	69

## List of table

<b>Chapter 1</b>	<b>Page</b>
1.1 Substrate materials for optical integrated circuits	3
<b>Chapter 2</b>	
2.1 Summary of dopants effect in pure silica glass	12
2.2. Typical soot deposition and waveguide fabrication method in silica layer and rare-earth incorporation for silica waveguide.	22
2.3 Typical fabrication method in silica layer and rare-earth incorporation for silica fiber.	22
<b>Chapter 3</b>	
3.1 Composition of elements in silica soot layer of pre-sintering temperature 950°C after solution doping for beam area A and C.	33
<b>Chapter 4</b>	
4.1 Diameter of circle and ring width in one cycle	51
4.2 Diameter of circle and ring width in multiple cycles	54
4.3. Diameter of circle varied with volume of droplets	63
4.4. Diameter of circle and ring width in multiple cycles by using pipette	66
4.5. Diameter of circle varied with temperature	66

## Abbreviations

B	Boron
B <sub>2</sub> O <sub>3</sub>	Borate glass
CVD	Chemical vapour deposition
EDFA	Erbium doped fiber amplifiers
EDWA	Erbium doped waveguide amplifier
EDX	Energy dispersive X-ray
Er <sup>3+</sup>	Erbium ion
ErCl <sub>3</sub> .6H <sub>2</sub> O	Erbium chloride
FESEM	Field emission scanning electron microscopy
FHD	Flame hydrolysis deposition
GaAs	Gallium Arsenide
Ge	Germanium
IC	Integrated circuit
InP	Indium Phosphide
LAN	Local-area-network
M	Molar
MAN	Metropolitan-area-network
MCVD	Modified chemical vapour deposition
N <sub>2</sub> O	Nitrogen dioxide
OFA	Optical fiber amplifier
OPA	Optical parametric amplifiers
P	Phosphorus
PECVD	Plasma enhanced chemical vapor deposition
RF	Radio-frequency
RIE	Reactive Ion Etching
SEM	Scanning electron microscopy
SiH <sub>4</sub>	Silane
Si-O	Silicon-oxygen bond
SiO <sub>2</sub>	Silicon dioxide
SOA	Semiconductor optical amplifiers
σ <sub>em</sub>	Stimulated emission

## **Chapter 1**

### **1.1 Optical telecommunication**

Modern optical based telecommunication was first introduced over 40 years ago around the 1960s. Optical telecommunication can be explained as the use of light signal to exchange data or information over a distance. Since the large-scale adoption of optical communication system began around the 1980s, there is a remarkable improvement of capabilities in this field. In pre-1980s, systems operated at data rates less than 150Mb/s in a length in the order of 10 km and carried at the most 30000 telephone channels. However, technology improvement in optical telecommunication continued. The system capacity expanded up to 480000 simultaneous telephone channels resulting from the innovation of dispersion shifted fiber and dense wavelength division multiplexing (DWDM) [1, 2].

The next important revolution in optical telecommunication technology is the optical amplifier. In a long haul data transmission stage, the optical signal becomes gradually weak as a result of scattering and dispersion. In order to maintain the light signal intensity, optical amplifier is needed to avoid any data transmission loss. Mainly, we have three kinds of optical amplifiers. They are optical fiber amplifiers (OFAs) which include erbium doped fiber amplifiers (EDFAs), rare earth amplifiers (REFAs) and Raman fiber amplifiers (RFAs), semiconductor optical amplifiers (SOAs) and optical parametric amplifiers (OPAs) [2, 3]. The minimum attenuation found in the 1550 nm window (which is coincidentally within the gain bandwidth of EDFAs), coupled with dispersion compensation techniques, allowed higher data rates to be carried over longer distances. EDFAs were used to permit repeater spacing's as large as 400 km and the overall system length was increased to 10000 km [2]. This

improvement is a technological breakthrough to the performance of telecommunication system. It overcomes the bit rate limitations in electrical systems and allows non-repeated length to increase ten-fold [1].

## **1.2 Integrated optics**

In 1969, S.E. Miller introduced the concept of integrated optics [4]. The term integration means combination of passive and active optical components on a common planar substrate either single or multiple materials [1, 5-7]. The optical components include splitters, sources, couplers, isolators, gratings etc. These components are fabricated on a planar substrate such as silicon. For example, an erbium-doped fiber amplifier (EDFA) is composed of many discrete parts such as isolator, pump and coupler. They usually are fiber based and these components are manually spliced together during the final assembly. By replacing the bulk optics with integrated optics, one can eliminate assembly steps which form all the waveguide on silica layer on a single substrate.

Integrated optics is the key towards low cost technology in fabrication optical components. In general, integrated optics can be grouped in two: monolithic and hybrid integration. Integrating multiple components and functions into a single material substrate is called monolithic integration [5]. Monolithic offers components coupling within a single, physically unique substrate which creates stable and highly compact multifunctional devices. This will overcome the coupling problem between various material components that is present in conventional bulk components. Besides that, the reduction in the number of optical components packaging also results in significant cost reduction. All the optical components including lasers as light source, detector, and modulators are formed in a same material substrate. In the case of active material, the



main choice for substrate is gallium arsenide or others in groups III-IV or II-VI. Since coupling of external light source such as laser is available, passive material can also be use as substrate materials. Table 1.1 shows the substrate materials used for optical materials. Indium Phosphorus (InP) is a promising substrate material in monolithic integration [5, 7]. To date, only InP as a substrate material that is able to provide integration of passive and active devices and operate in the 1310nm and 1550nm telecom windows.

Table 1.1. Substrate materials for optical integrated circuits [2]

Passive (Incapable of generation of light)	Active (capable of generation of light)
Quartz	Gallium arsenide
Lithium niobate	Gallium aluminum arsenide
Lithium tantalite	Gallium arsenide phosphide
Tantalum pentoxide	Gallium indium arsenide
Niobium pentoxide	Indium Phosphorus
Silicon	Other III-IV & II-VI
Polymers	
Silica	

However, some of optical devices can only be fabricated on different substrates and connected either directly or using optical fiber attached into the integrated circuit [7]. Hybrid integration means different optical components from various materials substrates being integrated to perform a specified task.

### 1.3 Optical amplifiers

. Optical amplifier is an active device which can regenerate or control the intensity of light signal. Erbium doped glass is used for the active waveguides. Analogous to the fiber amplifier structure and fabrication method, erbium doped waveguide amplifiers (EDWAs) are now being developed. The difference between EDFA and EDWA is pump efficiency. The doping concentration in EDWAs required

approximately 10-20 times than fiber. In high doping concentration, quenching effects occurs at high pump level results the pump efficiency drop [8]. Controlling between rare-earth doping and pump efficiency is needed to achieve a good performance in amplifier. Instead of pump efficiency, the waveguide losses are much higher than fiber. The pump power level in EDWAs required as much as twice reaching output powers on parity to an EDFAs. Another solution to high loss in waveguide is integration pump into waveguide without an intermediary fiber.

#### **1.4 Aim of research/ objective:**

The aims of the project undertaken consist of depositing fabrication silica soot layer by flame hydrolysis deposition (FHD) and investigate a method to incorporate erbium ion into the layer for the purpose of fabrication of optical amplifier. We successfully demonstrate non-selective area and selective area solution doping by syringe and pipette to deliver rare earth salt solution onto Germanium-silicate samples. The main key points included in our research:

- To determine the method to incorporate erbium ion into silica soot layer by dipping germanium-silicate samples into a rare-earth solution. This is called non-selective area doping. In addition, selective area doping is achieved by applying rare earth droplets onto similar samples using syringe and pipette.
- To investigate the variation in different pre-sintering temperature related to the incorporated erbium ion concentration in non-selective area doping. Surface morphology in different pre-sintering temperature is characterized and the number of pores per square area in silica soot layer is calculated by image J.
- To identify the doping duration of saturation point in order to optimize the process.

- To investigate dopant levels (molarity) incorporated into the silica soot layer in order to access the viability of method.
- Investigate the distribution concentration erbium ion in selective area doping via distance in selective doping area and also the spread diameter of doping area in different approaches (syringe and pipette) and method (one or multicycle).

## **1.5 Outline of thesis**

The first chapter provides an overview of optical telecommunication and integration optics.

Chapter 2 presents an introduction to glass structure, host composition effect to rare-earth doping level and fabrication method for silica-on-silicon such as PECVD, sputtering, sol-gel and ion implantation. The details about silica-on-silicon integrated optics and flame hydrolysis deposition (FHD) in fabrication silica soot layer is also discussed.

Chapter 3 focuses on solution doping method called non-selective area doping and also its principles are shown. Besides, the theory about transition energy in erbium can explained for more information about rare-earth doped amplifier. By the way the results and discussion about non-selective area doping in variation of pre-sintering temperature, molarity and dipping duration is showed.

In Chapter 4, the discussion on the novel selective area dipping is presented. The results showed the spread diameter of doping area and distribution concentration of erbium ion in various number of droplets in one cycle or multicycle dripping. Different substrate temperature by using hotplate also varied in selective area doping by pippette.

Lastly, the summary of thesis is presented. Conclusions are drawn and future works are suggested in chapter 5.

### **Reference:**

- [1] S. P. Watts, in Electronics and computer science (University of Southampton, 2002), p. 238.
- [2] R.G.Hunsperger, Integrated Optics: Theory and Technology (Springer, New York, 2002), p. 441.
- [3] B.E.A.Saleh, and M.C.Teich, Fundamentals of photonics (John Wiley & Sons,Inc, New Jersey, 2007), p. 1161.
- [4] S. E. Miller,"Integrated Optics: An Introduction," Bell Syst. Tech. J., vol **48**, pp.2059, 1969.
- [5] S.V.Frolov, T.M.Shen, and A.J.Bruce,"EDWA:Key Enabler of optical integration on PLC," rare-earth-doped materials and devices VII, vol, pp.47, 2003.
- [6] D. A. Guilhot, in Faculty of Engineering, Science and Mathematics, Optoelectronics Research Centre (University of Southampton, 2004), p. 165pp
- [7] L. Gines, in Integrated Photonics: Fundamentals2004), pp. 1.
- [8] D. R. Zimmerman, and L. H. Spiekman,"Amplifiers for the masses: EDFA, EDWA, and SOA amplifiers for metro and access applications," Lightwave Technology, Journal of, vol **22**, pp.63, 2004.
- [9] M. C. P. A. Dhar, M. Pal, A. K. Mondal, S. Sen, H. S. Maiti, and R. Sen,"Characterization of porous core layer for controlling rare earth incorporation in optical fiber," Opt. Express, vol **14**, pp.9006, 2006.

## **Chapter 2 Theory and Fabrication of Silica Layers**

### **2.1 Silica-on-silicon technology for integrated optics**

There are several available waveguide definition techniques for planar optical devices. Photolithographic and ultra-violet writing techniques are among these. In addition to waveguide formation techniques, there are a variety of substrate materials that are used in the fabrication of integrated optics devices. For instance, polymer [1], semiconductors compounds such as indium phosphide (InP) [2], or gallium arsenide (GaAs) [3, 4] have been produced in various application of optical devices. Another interesting substrate material is silicon-on-insulator technology but the scope of application of this technology is limited [5]. Among the above material platforms, silica-on-silicon substrate represents a much more versatile and mature technology used in the fabrication of planar waveguide [6-8]. One of the advantages in silica-on-silicon technology is in the use of the same material as optical fiber. This reduces fusion splicing problem between two kind of materials during assembly [9]. In addition, silica represents a durable and stable material that can accurately control refractive index between core and cladding layers. The optical loss is much lower in silica than soft glasses or polymers, resulting in silica being utilized in major parts of an optical network [7]. Besides that, silica-on-silicon fabrication technique was derived from the mature micro-electronics industry [8, 10], resulting in low production cost.

Typically, waveguide structures in silica-on-silicon consist of three types called rib, ridge and buried waveguide, as illustrated in Figure 2.1. All of the waveguide structures physically present in three layers. They are core, undercladding and overlcladding layer. The core layer normally was doped to increase refractive index compared to undercladding and overlcladding layers. The dopants used in the core layers depend on the application devices such as germanium to give rise refractive index,

boron used to reduce process temperature. The core layer confines and guides light to propagate through the waveguide. Photolithograph is used to pattern the core layer. The typical thickness of the core layer is in the range of 1 to 10  $\mu\text{m}$  [11]. The cladding layers are thicker than the core so as to isolate the guided light from the high index silicon wafer.

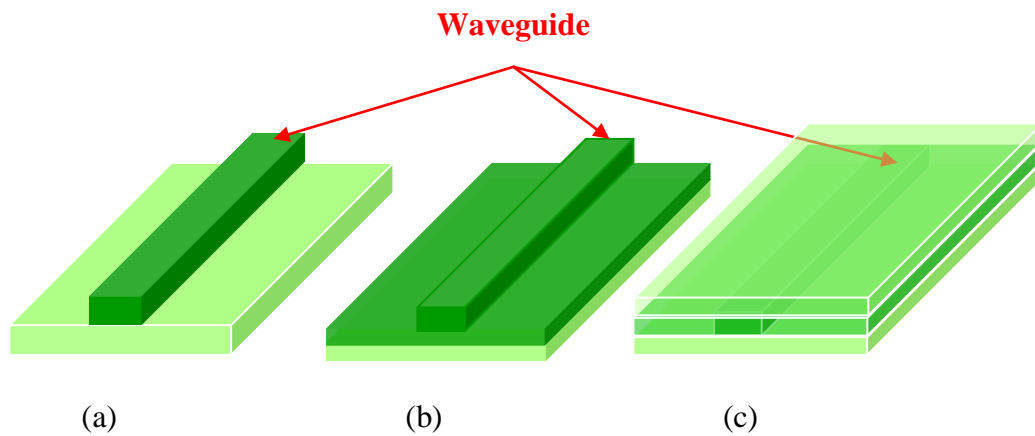


Figure 2.1 Three types of planar waveguides: (a) rib (b) ridge, and (c) buried

## 2.2 Doped glass structure and properties

Glass is in amorphous form. Amorphous is a state between crystalline solid and a liquid. In fact, glass exists naturally as crystals such as quartz, cristobalite and tridymite. When it is heated to a high temperature and cooled rapidly from liquid, the crystalline arrangement is broken. A form of glass called vitreous silica is formed [7, 12]. Physically glass possesses a short range order and also forms a three-dimensional matrix. However, glass structures lack uniformity, symmetry and structure of the crystalline material, having no long range periodicity [13]. Basically, glass called vitreous silica comprises one  $\text{Si}^{4+}$  ion and four  $\text{O}^{2-}$  ions.  $\text{SiO}_2$  is the principal component in glass. The pure silica structure has one silicon atom in the centre and forms covalent bonds with four oxygen atoms. The arrangement of oxygen atoms to silicon atom in silica glass structure is a three-dimensional tetrahedral form. The oxygen atoms are arranged tetrahedrally around the silicon atom as shown in Figure 2.2(a). This structure is similar

to the crystalline form of silica named cristobalite. A two dimensional diagram was showed in Figure 2.2(b). Zachariasen [12] formulated four requirements for the formation of glass. The requirements are:

1. Oxygen atom only can link to not more than two glass-forming atoms.
2. The coordinate number of glass forming ions must be small.
3. The polyhedral formed by oxygen must only share corners and not edges or faces.
4. The polyhedral must form a three-dimensional network.

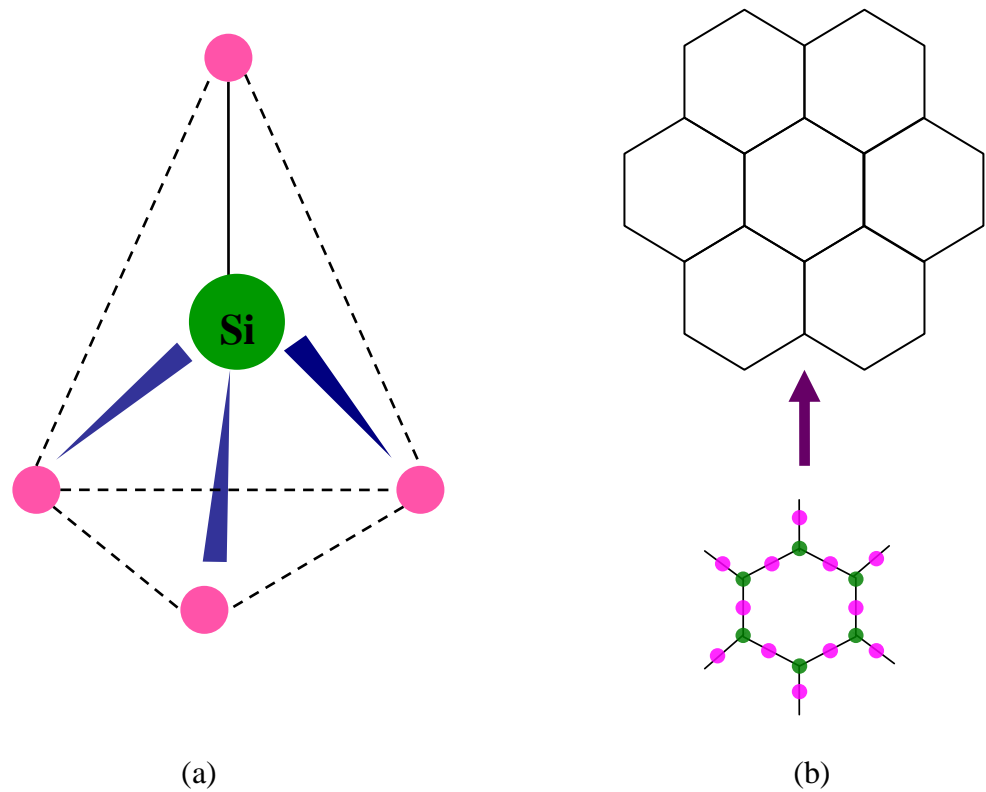


Figure 2.2 (a) schematic of three-dimensional tetrahedral arrangement in fused silica glass. (b) a diagram of two-dimensional matrix of silicon and oxygen atoms.

As described above, the pure silica glass is a rigid structure existing and lack of non-bridging silicon-oxygen bond ( $\text{Si-O}^-$ ) groups. In fact, non-bridging  $\text{Si-O}^-$  is important to allow for incorporation of rare-earth ions. The lack of non-bridging  $\text{Si-O}^-$  group makes low solubility of rare-earth ions [9]. According to rare-earth incorporation mechanism, the erbium ions will deposit into porous silica layer when the solvent evaporates. Subsequently, consolidation of glass will trap them inside the glass [7]. If

the concentration of rare-earth is low, the ion will be isolated and no effect to other rare-earth ions. As the concentration increased, the distance between ions will become smaller and the ions interactions give rise to concentration quenching [7, 13, 14]. This encourage for development of multi-component silicate and phosphate glass. A modifier atom is introduce into silica to open up silicon-oxygen structure or add an element to directly replace some of the glass forming atoms in the matrix so-called multi-component structure. Physically the additional dopants into glass layers lead to Si-O-Si bonds breaks, enabled incorporation of several weight percents of rare-earth ion without clustering. Clustering is extremely harmful, reducing radiative transitions in optical devices. Figure 2.3 showed the silica glass matrix disrupted by the addition of modifier ions [12].

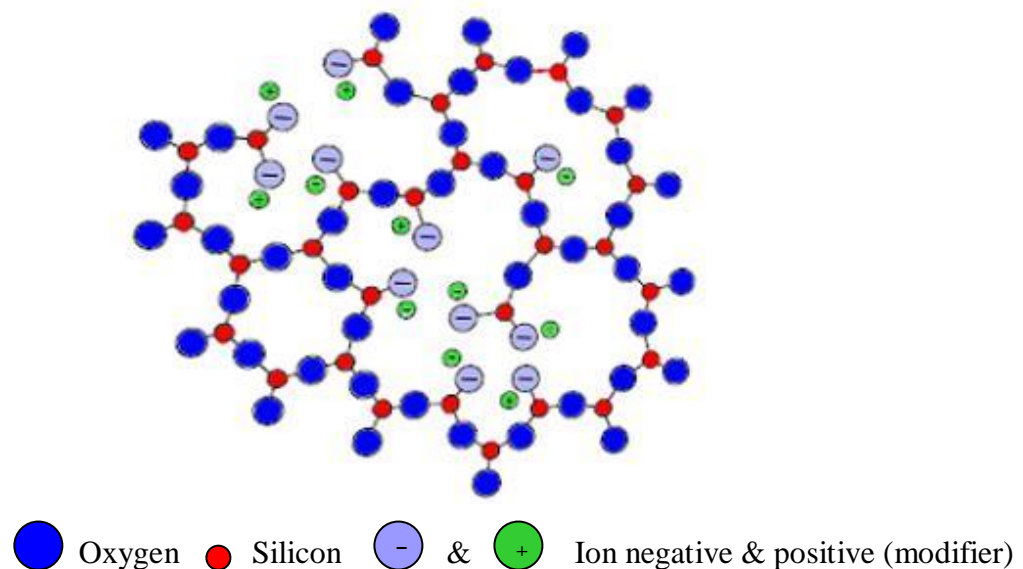


Figure 2.3 A schematic showing the silica glass matrix disrupted by the addition of modifier ions

### 2.3 Glass host composition

The glass host composition affects the solubility of the rare earth ions in silica core layer. Additionally, it may affect the fluorescence lifetime, absorption, emission and excited state absorption cross sections of the rare earth transitions. In fact, the adding of dopants such as germanium (Ge), phosphorus (P) and boron (B) into silica



glass layer gives a prevalent effect to solubility of rare earth incorporation. Meanwhile the dopants alter the properties of silica glass layers such as melting point, thermal expansion and refractive index. As mentioned above, the glass host is compatible with high concentration of rare-earth oxide without clustering requires the open, chain-like structure which can be created by adding modifier ions such as phosphorus, germanium, or boron [15]. The limitation owing to clustering in a predominantly silica host without modifier ions has been well documented [14]. In order to achieve high gain in Er-doped planar optical amplifiers, high concentrations of rare-earth ions are required. However, the maximum erbium concentration in silica for optimum amplifier performance has been suggested to be under 100 ppm [15, 16] to prevent clustering.

Consolidation temperature and refractive index can be altered by changing different proportions of dopants in silica core layer. However, the interrelationships between dopants are complicated and altering when additional two or more dopants are added into the silica glass layer. For instance, boron alone tends to decrease the refractive index and melting point of glass. Borate glass ( $B_2O_3$ ) is trivalent forms. Boron atom bonds to neighbouring oxygen atoms. With additional phosphorus and boron added together into the glass layer, the resultant layer may have a higher refractive index than the equivalent boron free layer [17]. The effects of the dopants used are summarized in Table 2.1.

Table 2.1 Summary of dopants effect in pure silica glass

Dopants	Chemical reaction	Effect
Germanium	Germanosilicate glass (SiO <sub>2</sub> : GeO <sub>2</sub> ) $\text{GeCl}_4 + \text{O}_2 \rightarrow \text{GeO}_2 + 2\text{Cl}_2$	Thermal expansion: increase; Glass melting point: decrease; Refractive index: increase
Phosphorus	Phosphosilicate glass (SiO <sub>2</sub> :P <sub>2</sub> O <sub>5</sub> ) $2\text{POCl}_3 + 2\text{H}_2\text{O} \rightarrow \text{P}_2\text{O}_5 + 6\text{HCl}$	Thermal expansion: increase; Glass melting point: decrease; Refractive index: increase
Boron	Borosilicate glass (SiO <sub>2</sub> :B <sub>2</sub> O <sub>3</sub> ) $4\text{BCl}_3 + 6\text{H}_2\text{O} \rightarrow 2\text{B}_2\text{O}_3 + 12\text{HCl}$	Thermal expansion: increase; Glass melting point: decrease; Refractive index: decrease

## 2.4 Principle of optical amplifier

Erbium doped waveguide amplifier is planar analogy of the erbium doped fiber amplifier. The EDWA operates with the same principle as erbium doped fiber amplifier (EDFA). As mentioned earlier, the optical signal is guided in a higher refractive index of core layers surrounded by a lower refractive index cladding layer.. The presence of erbium ion, Er<sup>3+</sup> has a specific spectroscopic feature with a strong radiative transition in the 1.54 μm wavelength region. It matches with the operation bandwidth of the third window in optical telecommunication system. Majority of erbium ions found in the ground state are in thermodynamics equilibrium. Using an external laser, the erbium ions are excited into a higher energy level where the population inversion is fulfilled. The condition of population inversion assumes more than half of the Er<sup>3+</sup> ions sit in the higher level. The energy level diagram of a free Er<sup>3+</sup> ion is shown in Figure 2.4.

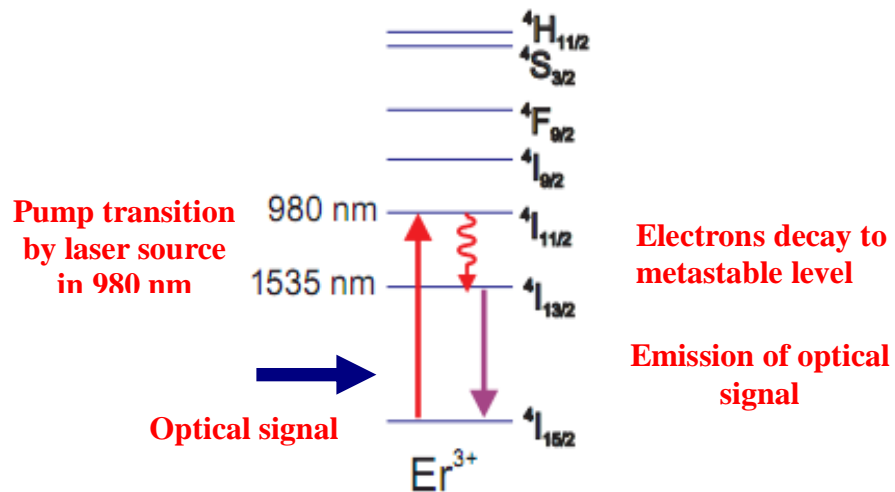


Figure 2.4 Energy level diagram of a free  $\text{Er}^{3+}$  ion [18].

The first excited state denoted as  ${}^4\text{I}_{13/2}$  is metastable and enables a laser transition to the ground state peaking at the wavelength of  $1.54 \mu\text{m}$  [18]. 980nm and 1480nm pumping wavelengths are usually employed as external laser source to excite the  $\text{Er}^{3+}$  ions into a higher energy level. Erbium ions can directly be pumped into the first excited manifold,  ${}^4\text{I}_{13/2}$  by using laser operating at the wavelength of 1480 nm or excited into a higher energy level,  ${}^4\text{I}_{11/2}$  by using 980 nm pump.  $\text{Er}^{3+}$  ions at  ${}^4\text{I}_{11/2}$  will decay rapidly to a long-lived energy level at  ${}^4\text{I}_{13/2}$  called metastable state. The lifetime in metastable state is about 10 ms. The optical signal amplification process takes place when  $1.54 \mu\text{m}$  optical signal photon traveling through the active medium. The optical signal photon stimulates the emission of a second photon, having the same frequency, phase, polarization and direction of propagation as the original one. Besides stimulates emission mention above, relaxation of  $\text{Er}^{3+}$  ions can occur spontaneously. Spontaneous relaxation can occur either radiatively or nonradiatively. The radiative spontaneous emission produces photons with random phase, polarization and propagation direction. Furthermore, the spontaneous emission decreases the population inversion indirectly limits the amplifier gain.

## 2.5 Amplifier Properties and Parameters

**Erbium concentration and solubility:** The  $\text{Er}^{3+}$  ions concentration embedded in glass layer is an important parameter for amplification. The higher  $\text{Er}^{3+}$  ions concentration, the higher gain achieved for optical amplification. The maximum gain per unit length is determined by the product of cross-section for stimulated emission  $\sigma_{\text{em}}$  and the active Er concentration. Since typical values for  $\sigma_{\text{em}}$  are in the  $10^{-21}$ - $10^{-20}$   $\text{cm}^2$  range, concentrations of  $10^{19}$ - $10^{20}$   $\text{Er}/\text{cm}^3$  are required to achieve a reasonable gain over a length of a few centimeters [18, 19]. Therefore, the host material must have a high  $\text{Er}^{3+}$  ions solubility in silica layer. High solubility of  $\text{Er}^{3+}$  ions was achieved by multi-component in silica glass layer. Since pure silica form is rigid, various network modifiers were used to open up the structure of silica. The  $\text{Er}^{3+}$  ions incorporation increased showed by phosphorus in glass matrix [20, 21].

**Waveguide loss:** Waveguide loss is determined by the scattering and absorption when optical signal propagates in a waveguide. The signal loss may occur due to intrinsic elements has to be compensated by stimulated emission to achieve net amplification. The scattering may occur at rough waveguide edges or on material inhomogeneities and impurities. The incorporation of rare-earth ions can become the center of scattering. Moreover,  $\text{Er}^{3+}$  ions doped glass exhibit higher propagation loss than the undoped glass.

**Overlap factor:** In order to achieve optimum gain, the modes profiles are best to be overlapped perfectly where both signal and pump light should be confined in the waveguide. Subsequently, high population inversion coincides with the signal mode distribution to achieve high gain optical. For low refractive index contrast, part of optical signal travels through the cladding layers will obtain low gain.

**Co-operative and up-conversion:** Interaction between  $\text{Er}^{3+}$  ions is important in gain limiting effect. At high concentration of erbium doped, the erbium ions are close enough and accumulate together in silica porous layer. In this condition, the excited  $\text{Er}^{3+}$  ions in higher level,  $^4\text{I}_{13/2}$  decay by transferring its energy to its nearest neighboring excited ions. The neighboring ions lift up to a higher energy state,  $^4\text{I}_{9/2}$ . The erbium ion relaxes quickly through phonon interactions and back to metastable or directly to the ground level. This lowers the amount of excited  $\text{Er}^{3+}$  ions in the metastable level; inversely increase the pump power to maintain the population inversion.

## **2.6 Method for fabrication silica soot layer**

The process flow in our work includes thin film deposition and solution doping followed by consolidation in high temperature. The thin film deposition is where the silica layer is deposited on silicon substrate by using various techniques such as plasma enhanced chemical vapour deposition (PECVD) [8], sol-gel [22, 23] and flame hydrolysis deposition (FHD) [6-8]. Firstly, the source materials are provided in form of solid, liquid or vapour. Then the source is fed into the target of substrate where deposition of silica layer takes place. Subsequently the porous silica layer is annealed into a pre-sintering stage. The pre-sintering stage refers to a rigid form of porous silica soot structure where is used to solution doping. After solution doping, the samples were dried in room temperature and dehydrated in oven. Various methods were used to deposit silica layer on silicon substrate are described as following.

### **2.6.1 Flame Hydrolysis Deposition (FHD)**

The process of flame hydrolysis deposition (FHD) is a development of techniques used to deposit porous silica layer on silicon substrates in fabrication planar lightwave circuit. In the process, the vapor precursors are introduced into an oxy-

hydrogen flame where the oxidation and hydrolysis of vapor precursors are occurred. The vapor precursors included  $\text{SiCl}_4$  and others dopants which works as their own functional. The silicon tetrachloride can be oxidized or hydrolyzed in flame above  $1200\text{ }^\circ\text{C}$  to produce silica. The hydrolysis reaction is dominant in these reactions. The reactions are showed below:



Silicon tetrachloride is carried by helium gas using a bubbling system through the liquid form of the precursors. Helium gas is used as carrier gas as it is an inert gas and there are no chemical reactions occurring between carrier gas and precursors. The silicon tetrachloride is reacted with oxy-hydrogen flame, resulting the silica soot particles and hydrochloric acid are formed. The silica soot particles are deposited on silicon substrates and the gaseous chloride is extracted away. Figure 2.5 schematic the deposition of silica soot layer in FHD.

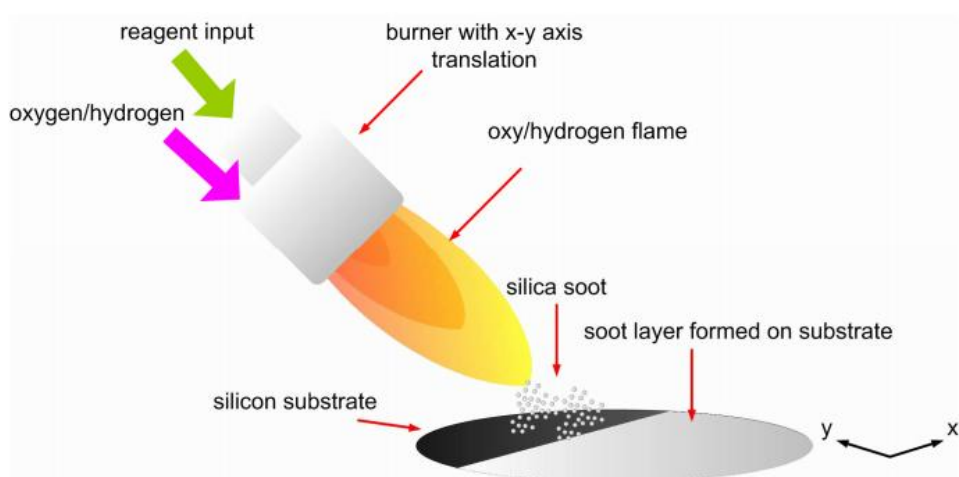


Figure 2.5 Schematic and photo of deposition step of FHD. The soot is then consolidated to form a glassy layer [8].

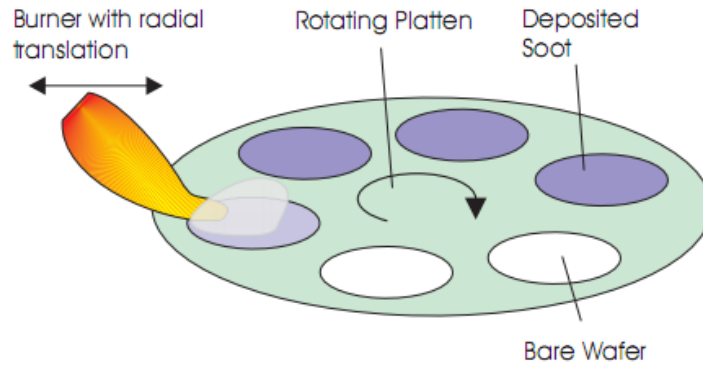


Figure 2.6 Schematic of burner's position and turntable rotate in flame hydrolysis deposition [6].

The vapour supply rate to the burner will control the thickness and the uniformity of deposition soot layers. The burner is moved translation relative to the substrate where the substrate is rotated on turntable as illustrated in Figure 2.6. A wide range of dopants can be used to tailor the composition of soot and therefore the final glassy layer. Typically phosphorous, boron and germanium can be added using halide compounds. The chemical reactions are show below:



By adding the dopants into silica layer give a change to properties of glass layer. The deposited silica soot layer then consolidates in high temperature exceeding 1200°C. One of the advantages of using FHD is the ease in controlling the deposited soot, and resulting consolidated film thickness, by controlling the gas precursor flow rate [7]. The thick soot layer deposited could also be incorporated with dopants using a solution doping technique [24-30] developed for the waveguide fabrication industry. Another advantage of FHD is that the samples fabricated display low stress formation during the

deposition step due to the interaction between soot particles (a weak interaction), as opposed to the atomic bonding mechanism taking place in alternative techniques such as those based on chemical vapour deposition (CVD).

### 2.6.2 Plasma Enhanced Chemical Vapour Deposition (PECVD)

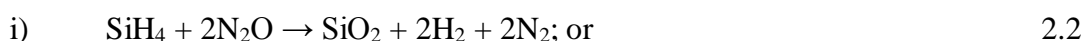
Plasma enhanced chemical vapour deposition (PECVD) is a thin film deposition technique by using radio-frequency (RF) or microwave energy to create plasma to deposit silica layer on silicon substrate. It used chemical vapour deposition techniques. Chemical vapours are deposited on a substrate by provoking chemical reactions in a deposition chamber at low pressure (0.2-1.0Torr). It is also an initial, low-temperature reactant gas reacts with other gases to give a solid phase deposit on the substrate surface.

The chemical reactions include in PECVD:

a) when oxygen is used:



b) when nitrous oxide is used:



In PECVD, a radio frequency discharge creates low-pressure plasma in an appropriate gas mixture for an initiate the reactions.  $\text{SiH}_4$  and  $\text{N}_2\text{O}$  is the most usual mixture used for PECVD [31]. Firstly, precursors in gas phase form are flowed into a deposition chamber and then the free electrons accelerated when applied electric field. The production of a plasma occurred when collisions of electrons are able to ionize the precursor molecules. The electrons acquire energy when collision occurred. The primary electrons acquire a high energy, some of which they lose by colliding with particles, giving ions and secondary electrons. Consequently, formation of free radicals



and ion are generated. The highly energy of free radicals and ions are incident onto the substrate where their energy is dissipated and adsorption takes place. The free radicals are absorbed by the layer. The atoms rearrange and diffused into the surface of substrate. A stable film is formed and followed by the annealing stage to densify the film formed. A schematic representation of the technique is shown in Figure 2.7 [8].

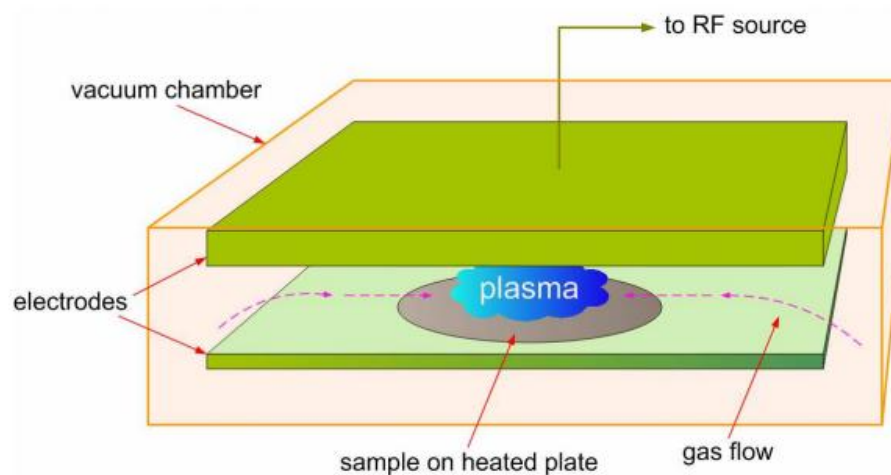


Figure 2.7. PECVD deposition chamber and process schematic.

PECVD has many advantages. It gives good uniformity silica layers in fact the deposition times are few hours. PECVD is a mature and proven technology used in deposition for microelectronic industry. The dopants can easily introduce into silica layers while producing high quality silica glass layer. The low temperature in processing is a great attractive requirement for PECVD compares to others deposition techniques. The glasses with volatile components such as phosphorus can be deposited, as it is a low temperature process.

### 2.6.3 Sol-gel

Sol-gel method is a fabrication of synthesis glass by chemical solution. It provides a simple low-cost route for fabricating dense smooth glass layers. Firstly, the sol is formed which is a colloidal suspension of solid particles in a liquid. Then the sol

turn into gel form which a semi solid two components system rich in liquid. The sol contains all the elements required to form a final glass matrix. The sol is prepared by adding the dopants precursors to a solvent such as alcohol in correct quantities, followed by a hydrolysis step using water. The sol is then applied to silicon substrate by spin coating to form a homogenous thin film. The particles in solution coalesce to form a thin film gel. The thin film gel contain all the elements include the dopants such as erbium and solvent. Subsequently, evaporation of solvent is done by heating in an oven called densification glass layer through annealing or sintering process. In the other way, the silica sol is prepared and coated on silicon substrate by using spin coater. Thin film is then doped by soaking in the salt solution, rinsed thoroughly in deionized water, and dried with a nitrogen gun. Lastly, the gel film was then baked in air in an electric tube furnace. A simple diagram of the sol-gel layer synthesis route for spin coating is showed in Figure 2.8 [22].

Sol-gel method is a simple, easy and low cost in silica glass fabrication. It gives a nanoscale porosity, high surface area and homogeneity on scale of optical waveguide [23]. However, cracking is a main problem faces by sol-gel method when drying process. The drying condition leads the problem in cracking, peeling of thin film results by non-uniform shrinkage. The deposition area must below 6-in wafers to produce a homogenous and low-porosity film [22].

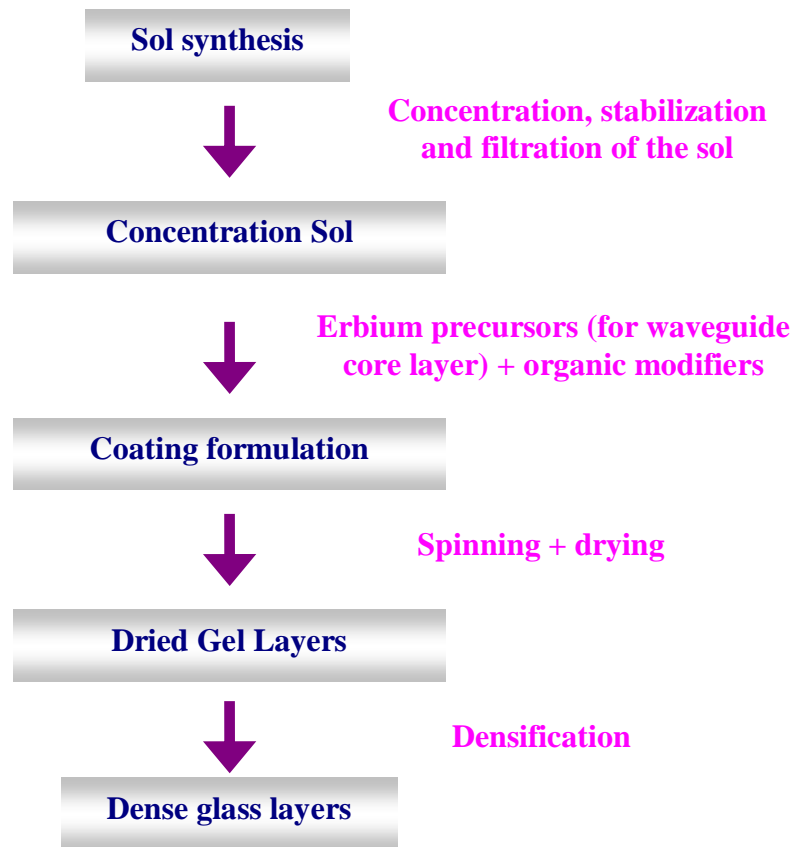


Figure 2.8. Diagram of the sol-gel synthesis route.

## 2.7 Review of solution doping

Solution doping is a rare-earth incorporation method into silica glass either in fiber or planar form. It is an easy and low cost process to incorporate rare-earth ion into silica porous layer and also used in silica fiber fabrication for optical amplifier and fiber laser. Recently, the research attention move forwards rare-earth doped planar waveguides due to intensive development technology of integrated optics. Solution doping method will be described in detail in the following chapter. The following are two tables giving a summary in typical soot deposition and waveguide fabrication method in silica layer and rare-earth incorporation for silica waveguide and optical fiber.

Table 2.2. Typical soot deposition and waveguide fabrication method in silica layer and rare-earth incorporation for silica waveguide.

Soot deposition and waveguide fabrication method	Material (Rare-earth incorporation)	References
1. Flame hydrolysis deposition 2. Reactive ion etching (RIE)	Neodymium (Nd)	[26, 32]
1. Modified chemical vapour deposition (MCVD) 2. Reactive Ion Etching (RIE)	Neodymium (Nd)	[20]
1. Sol-gel method 2. Reactive Ion etching (RIE)	Erbium (Er)	[22]
1. Flame hydrolysis deposition	Erbium (Er)/ Aluminium (Al)- co-doping	[33]

Table 2.3 Typical fabrication method in silica layer and rare-earth incorporation for silica fiber.

Soot deposition method	Material (Rare-earth incorporation)	References
1. Modified chemical vapour deposition (MCVD)	Aluminium (Al)	[27, 29, 34]
1. Modified chemical vapour deposition (MCVD)	Erbium (Er)/ Aluminium (Al) – codoping	[20, 28, 30, 35, 36]
3. Modified chemical vapour deposition (MCVD)	Erbium (Er)/ Ytterbium (Yb)-codoping	[24]

Table 2.1 showed that silica porous layer has been deposited by flame hydrolysis deposition (FHD), modified chemical vapor deposition (MCVD) and sol-gel process following by reactive ion etching to form silica waveguide. Rare-earth ion such as neodymium (Nd) and erbium (Er) are used to introduce into silica core layer to

fabricate optical amplifier. Co-doping i.e. aluminium was introduced as a function to reduce the clustering effect in the silica glass layer. By adding aluminium ions into silica network with a tetrahedral structure,  $[\text{AlO}_{4/2}]^-$ , these ions attract  $\text{Er}^{3+}$  ions to reduce free energy and prevent clustering of  $\text{Er}^{3+}$  ions. In optical fiber amplifier, modified chemical vapour deposition (MCVD) is the main choice method uses to fabricate perform fiber.

## 2.8 Summary

In this chapter, the advantages of silica on silicon technology have been reviewed. The doped glass structure and properties have been described and showed the structure in diagram. Besides, principle and parameter of erbium doped in amplifier have been explained. The techniques of fabrication methods for deposition silica porous layer also have been listed. Lastly, a review of solution doping with references have been presented.

### Reference:

- [1] R. T. Chen *et al.*, *Photonics Technology Letters*, IEEE **5**, 1328 (1993).
- [2] J. Schneider, M. Moser, and K. Affolter, in *Indium Phosphide and Related Materials*, 1994. Conference Proceedings., Sixth International Conference on 1994), pp. 216.
- [3] H. Yamada, H. Ito, and H. Inaba, *Electronics Letters* **20**, 591 (1984).
- [4] J. Jakobsen, in *Gallium Arsenide Integrated Circuit (GaAs IC) Symposium*, 1997. Technical Digest 1997., 19th Annual 1997), pp. 7.
- [5] P. D. Trinh *et al.*, *Photonics Technology Letters*, IEEE **9**, 940 (1997).
- [6] S. P. Watts, in *Electronics and computer science* (University of Southampton, 2002), p. 238.
- [7] D. A. Guilhot, in *Faculty of Engineering, Science and Mathematics, Optoelectronics Research Centre* (University of Southampton, 2004), p. 165pp
- [8] F. R. M. Adikan, in *Faculty of engineering, science & mathematics* (university of southampton, 2007).
- [9] B. J. Ainslie, *Lightwave Technology*, Journal of **9**, 220 (1991).
- [10] P. Heimala, and A. J. Aarnio, *Journal of Physics D: Applied Physics* **25**, 733 (1992).
- [11] S.V.Frolov, T.M.Shen, and A.J.Bruce, *rare-earth-doped materials and devices VII*, 47 (2003).
- [12] S. P. CRAIG-RYAN, and B. J. AINSLIE, edited by P.W.FRANCE (CPC Press, Inc, 1991), p. 259.

- [13] P.W.FRANCE, edited by P.W.FRANCE (CPC Press, Inc, 1991), p. 259.
- [14] F. Auzel, and P. Goldner, *Optical Materials* **16**, 93 (2001).
- [15] J. R. Simpson, *Rare-earth-doped fiber lasers and amplifiers* (Marcel Dekker, Inc, New York, 2001).
- [16] A.Polman, in *Proc. 10<sup>th</sup> European Conference on Integrated Optics (ECIO)* Paderborn, Germany, 2001), p. 4.
- [17] I. J. G. Sparrow, in *faculty of engineering, science & mathematics* (university of southampton, 2005).
- [18] J. Jagerska, in *physical electronics* (CZECH technical university, prague, 2005/2006), p. 74.
- [19] P.G.Kik, and A.Polman, in *MRS Bulletin* (FOM Institute for Atomic and Molecular Physics, The Netherlands, 1998).
- [20] B. Wu, and P. L. Chu, *Photonics Technology Letters*, IEEE **7**, 655 (1995).
- [21] M. C. P. A. Dhar, M. Pal, A. K. Mondal, S. Sen, H. S. Maiti, and R. Sen, *Opt. Express* **14**, 9006 (2006).
- [22] R. R. Thomson *et al.*, *Lightwave Technology*, Journal of **23**, 4249 (2005).
- [23] O.McCARTHY, and E.M.YEATMAN, *journal of sol-gel science and technology* **13**, 579 (1998).
- [24] J. E. Townsend, S. B. Poole, and D. N. Payne, *Electronics Letters* **23**, 329 (1987).
- [25] B. J. Ainslie, *Journal of Lightwave Technology* **9**, 220 (1991).
- [26] J. R. Bonar *et al.*, *Electronics Letters* **30**, 229 (1994).
- [27] F. Z. Tang *et al.*, *Journal of Non-Crystalline Solids* **352**, 3799 (2006).
- [28] A. Dhar *et al.*, *Optics Communications* **277**, 329 (2007).
- [29] F. Z. Tang *et al.*, *Journal of Non-Crystalline Solids* **354**, 927 (2008).
- [30] F. Z. Tang *et al.*, *Journal of Non-Crystalline Solids* **354**, 1582 (2008).
- [31] A. Sherman, *chemical vapor deposition for microelectronics: Principles, Technology, and applications*. (Noyes Publications, 1987).
- [32] Y. Hibino *et al.*, *Photonics Technology Letters*, IEEE **1**, 349 (1989).
- [33] S. I. Ro, Y. S. Jung, and D. W. Shin, *Journal of Ceramic Processing Research* **2**, 155 (2001).
- [34] F. Z. Tang *et al.*, *Journal of American Ceramic Society* **90**, 23 (2007).
- [35] A. Dhar *et al.*, *Opt. Express* **14**, 9006 (2006).
- [36] A. P. A. Dhar, M. C. Paul, P.Ray, H. S. Maiti, and R. Sen, *optics express* **16**, 12835 (2008).

## **Chapter 3 Solution doping**

### **3.1 Introduction to rare-earth doping techniques**

There are two main techniques used for rare-earth doping in silica layer formed by FHD. These are solution doping and aerosol doping. Solution doping of silica is a widely used technique to incorporate rare-earth ion into silica glass layer for amplification purpose. The solution doping process involves two major steps. The first step is deposition of silica porous core layer and annealing in pre-sintering stage. The pre-sintering stage refers to the deposition silica soot layer and then annealing in intermediate temperature below consolidation temperature to get a denser porous silica soot layer. Subsequently, the porous silica layer is immersed into rare-earth containing alcoholic or aqueous solution. The technique was developed for incorporation rare-earth ions in fibers and was then adapted to the planar format, mainly for the fabrication of lasers [1-3].

On the other hand, aerosol doping [4-6] involves incorporation of dopants into a burner by using an atomizer. The incorporation of aqueous rare-earth chloride into the burner during deposition involves a single step process. This can alleviate the complication of partial fusing; a necessary procedure for solution doping. The atomizer produces a monodispersed distribution of aerosol droplets which were then transferred to the burner. Water is then evaporated, leaving submicron particle of rare-earth. Oxidation of rare-earth particles takes place in oxy-hydrogen flame and distributed uniformly through the structure. Aerosol doping does not involve handling of soot layer resulting in a lower contamination of soot layer. This is the advantage offered by aerosol doping compared to solution doping. However, it is difficult to control the concentration and uniformity of dopants via this method.

### **3.2 Principle of solution doping**

As mentioned above, the principle of solution doping involves two major processes. The partially consolidated porous layer is deposited and then immersed into rare-earth containing alcoholic or aqueous solution. The rare-earth ions incorporation into soot layers includes two main mechanisms i.e. physically and chemical. Physically the soot acts as a sponge and takes up the solution by capillary action. The dopants are deposited in the pores when the solvent evaporates. The consolidation steps in high temperature will trap the dopants inside the glass layer. In this case, the porous silica soot layer produced with different pre-sintering temperature and different concentration of solution will affect the amounts of rare-earth incorporation. The chemical mechanism involves the bond formation between the dopants ions and the soot ions when doped in an aqueous solution. The atoms of dopants are chemically trapped in the silica porous layer. The rare-earth materials that have been used in solution doping are erbium [3, 7], ytterbium, neodymium [1, 8] etc. Others dopants such as aluminium is also used in solution doping to decrease the clustering effect in silica waveguide [3, 9]. In our work, we used erbium as the dopant.

### **3.3 Experimental method**

In this work, flame hydrolysis deposition (FHD) was used to deposit layers of silica ( $\text{SiO}_2$ ) soot onto standard 4-inch silicon substrates. A modification of existing standard FHD process is introduced in the form of an additional stage where incorporation of rare earth elements into a pre-sintered porous core layer is performed. In general, silica soot layer samples will be fully consolidated to form a dense glass layer at temperatures around  $1320^\circ\text{C}$ . To allow for incorporation of rare earth elements through solution doping, the deposited soot layer would first undergo a pre-sintering stage, followed by full consolidation after solution doping. Pre-sintering in this case



refers to heating the soot layer to a temperature that would result in the layer being semi-consolidated. This will create a sufficiently high porosity layer to facilitate water absorption while retaining surface integrity i.e. the pre-sintered layer does not peel off or crack in subsequent processing. In essence, the porous silica acts as a sponge, taking up the solution and the mechanisms taking place during this are capillary action and chemical absorption [2, 10, 11]. Therefore, the porosity of the silica layer, which is determined by the pre-sintered temperature, takes an important role to ensure a sufficient concentration of rare-earth impregnation [12-14]. Besides, the rare earth solution concentration, and dipping duration are also important factors that need to be considered [15].

The pre-sintered samples would then be completely immersed in a rare earth solution, in this case 0.1M erbium chloride hexahydrate ( $\text{ErCl}_3 \cdot 6\text{H}_2\text{O}$ ) aqueous solution, for 1 hour. The doped samples are then dried at room temperature for 30-60 minutes followed by a dehydration phase involving oven heating at  $100^\circ\text{C}$  for 30 minutes before being fully consolidated. Due to the isotropic nature of solution diffusivity into a porous layer, this process will result in a core layer being fully doped with rare earth, hence the term non-selective area doping. For pre-sintering temperature samples, samples were heated at temperatures between  $750^\circ\text{C}$  to  $950^\circ\text{C}$  for 45 minutes. The optimum pre-sintering temperature would produce a layer with good surface morphology and adhesion to the base silicon substrate. In non-selective area doping, dipping duration and molarity were used to vary the erbium ion incorporation in silica layer. The number of pores per square area and thickness of silica porous soot layer was also investigated and analyzed by using image J. The images are either captured from SEM or microscope optic. For variation of molarity, the pre-sintering samples (silica soot layer) were dipped in erbium chloride ( $\text{ErCl}_3 \cdot 6\text{H}_2\text{O}$ ) aqueous solution which was varied from

0.02-0.10M [15, 16]. The dipping duration of silica soot samples in the aqueous solution was investigated from 5 to 80 minutes in order to determine a saturation point in dipping time. Energy dispersive X-ray (EDX) was used to study erbium concentration incorporation into soot layer for different molarity and dipping duration. Refractive index in different molarities samples was measured by a prism coupler system (SAIRON Tech. SPA-4000).

### **3.4 Principle of Pre-sintering of soot layer**

The raw soot deposited by flame hydrolysis deposition (FHD) is fragile and easily damaged before pre-sintering stage. Hence, the FHD soot needs to be pre-sintered in order to strengthen the matrix. The mechanism responsible for consolidating FHD soot into fully densified glass layer is called viscous sintering. In this case, consolidation of FHD soot layer occurs after solution doping. Pre-sintered of raw soot layer is heated to near their melting point before the solution doping step in order to get a strengthen form of soot layer. The soot particles assume as circle form and tend to be spherical during the FHD process. In this time, the particles form a tenuous network containing pores. They adhere together through molecular forces. When heating the raw soot layer in intermediate temperature called pre-sintering stage, resulting in the growth of a “neck” between adjacent particles. The separation for centre-to-centre of two particles reduces like illustrated in Figure 3.1. This effect is attributed to surface tension. A skeleton of glass matrix is formed induces an increase in particle size and pore size as the pores agglomerate during pre-sintering process. The raw soot produced by FHD has a very open structure as mention above. The necking effect results in a gradual closure of open structure between spheres and the formation of pores. These pores provided surface tension effects that produces a capillary pressure which responsible to take up the rare-earth ions during solution doping. Hence, if the pre-sintering temperature is too

close to the consolidation temperature, the glass matrix will fused together. The incorporated dopants in silica porous layer will isolate and resulting non-uniform doping.

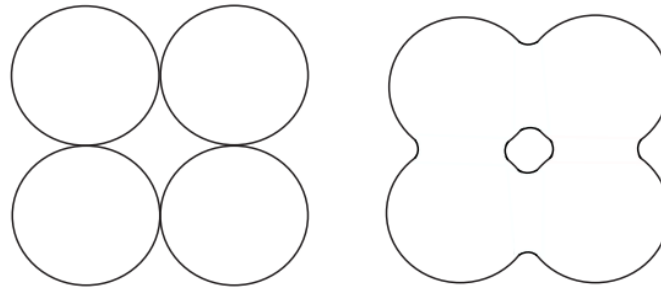


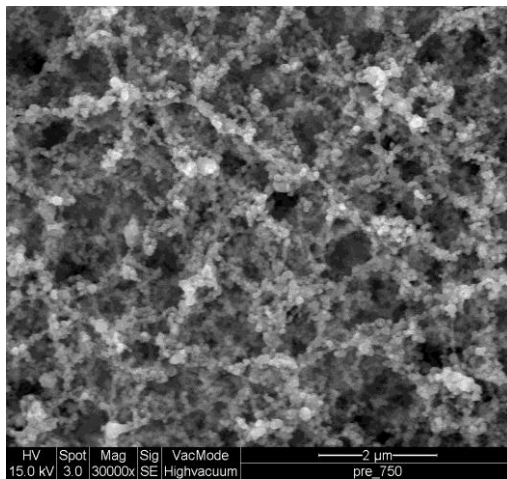
Figure 3.1 Necking of particles during pre-sintering process

### 3.5 Pre-sintering soot layer

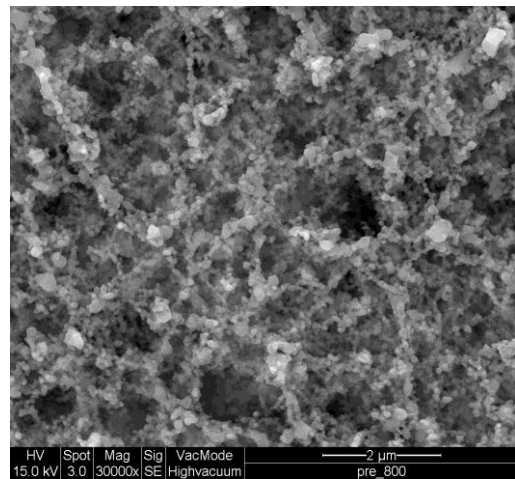
The mechanism for the formation of silica soot layer has been explained in the above section. The porous soot layer has been investigated in different pre-sintering temperature to determine agglomeration of particles as temperature changed. Field emission scanning electron microscopy (FESEM) was used to show the agglomeration of particles in different pre-sintering temperature. The microstructure and morphology of silica porous layer were studied; the results shown in Figures 3.2 (a)-(e) for pre-sintering temperatures between 750°C-950°C. Comparison of the FESEM images indicates that the network formation and pore sizes distribution are influence by temperature. The structure of glass matrix indicates a clearer and bigger pore size distribution in network formation of soot particles for higher temperature i.e 950°C compares to that lower of temperatures. At high temperatures, the structure of glass matrix is more rigid and stronger than at low temperature. During soot deposition, the particles adhere together through molecular forces, resulting in the formation of silica network. Increase in the necking effects results in the size particles becomes bigger when temperature increases [4, 16]. This leads to the partial fusing of silica layer that

becomes larger as the silica particles agglomerate. Hence the pore size increases. The silica porous layer becomes denser due to necking affect.

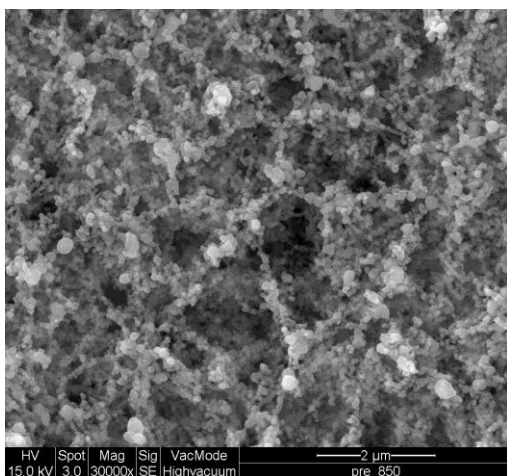
Figure 3.3 (a)-(e) show the microstructure and morphology of silica porous layer after solution doping in 0.1M erbium chloride ( $\text{ErCl}_3 \cdot 6\text{H}_2\text{O}$ ) aqueous. There is a significant difference between the morphology of silica soot layer before and after solution doping. The images show the agglomeration of particles fluffy after being soaked in solution. However, the pores size distribution still become larger as the deposition temperature increased. The deposited soot layer is fluffy and no discernible difference in appearance at temperature  $750^\circ\text{C}$  to  $900^\circ\text{C}$  while the deposited at  $950^\circ\text{C}$  is more compact in appearance [2, 17].



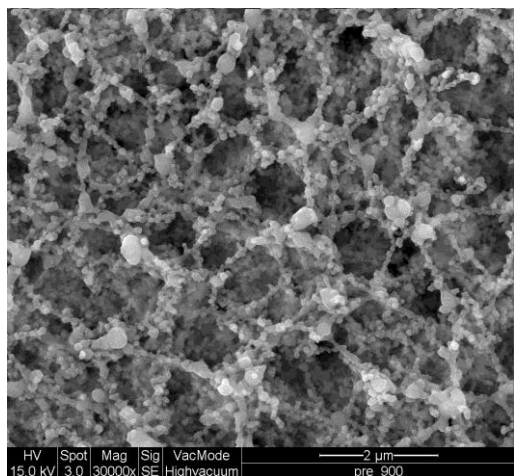
(a)



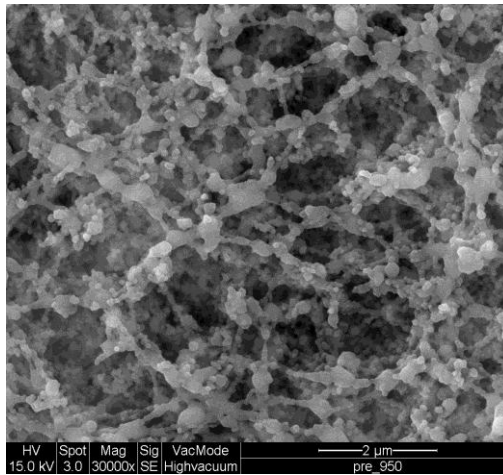
(b)



(c)

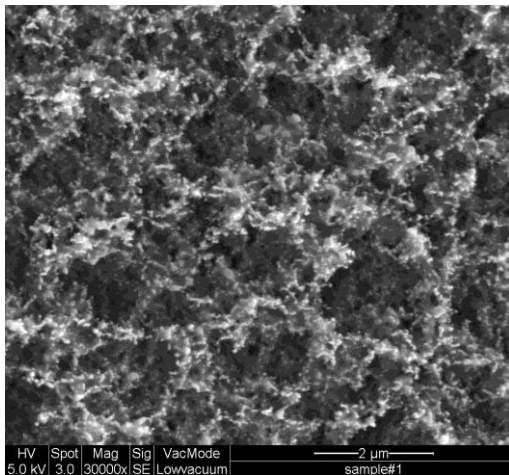


(d)

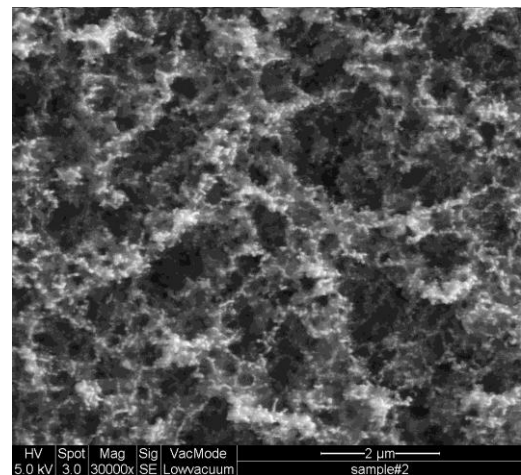


(e)

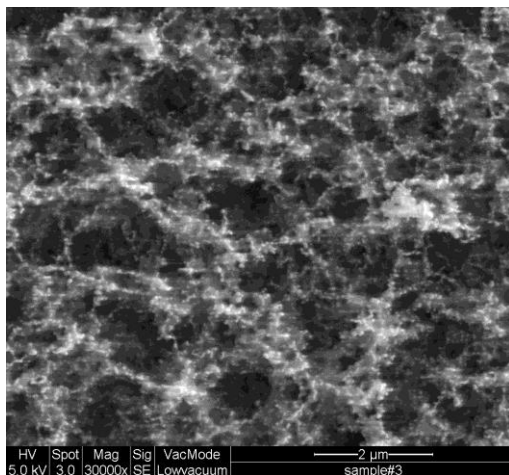
Figure 3.2 FESEM images: The morphology and microstructure of silica soot layers at different pre-sintering temperatures before solution doping with magnification 30k x. (a) 750°C (b) 800°C (c) 850°C (d) 900°C (e) 950°C



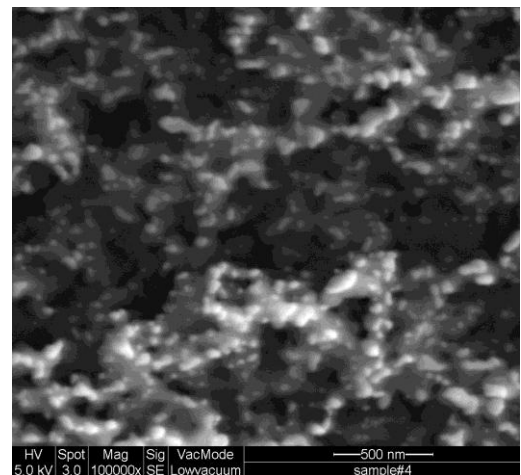
(a)



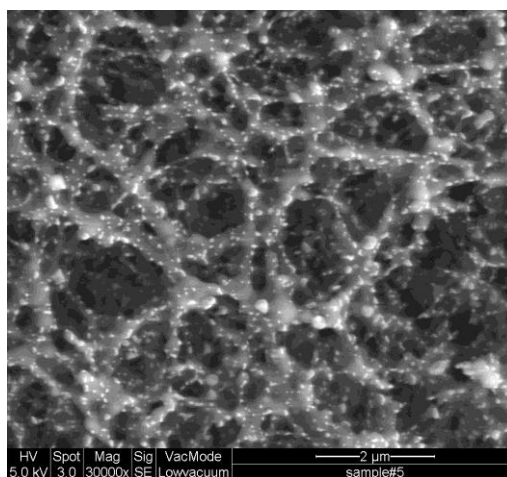
(b)



(c)



(d)



(e)

Figure 3.3 FESEM images: The morphology and microstructure of silica soot layer at different pre-sintering temperatures after 0.1M erbium chloride ( $\text{ErCl}_3 \cdot 6\text{H}_2\text{O}$ ) aqueous solution doping with magnification 30kx. (a) 750°C (b) 800°C (c) 850°C (d) 900°C (e) 950°C

There are significant amounts of white particles distributed throughout the layer. EDX was used to determine the white particles in the silica soot layer in pre-sintering temperature 950°C after solution doping. The X-ray beam was injected into two areas, i.e. white particles area and no white particles area to differentiate the material composition. The beam size of the EDX is 1 nm. From the energy dispersive X-ray (EDX) results, we cannot define the composition of material in white particles. Comparison between the white particles area and no white particles area, the EDX results show that aurum and carbon are the most suspected materials. In my opinion, these two materials cannot define the white particles. The presence of aurum (Au) in the soot particle is a result of aurum coating for soot particle when characterized by EDX. Silica soot layer is not an electrical conductive specimen. Nonconductive specimens will cause accumulation of electrostatic charge at the surface, which will give fault scanning. Phosphorus (P) and germanium (Ge) are the contents of the silica soot layer. However, the presence of carbon (C) is suspected to come from contamination contents of samples. Figure 3.4 shows the area of beam injection to the silica layer by EDX. Table 3.1 shows the composition of elements found in the silica layer for two areas, i.e. A and C.

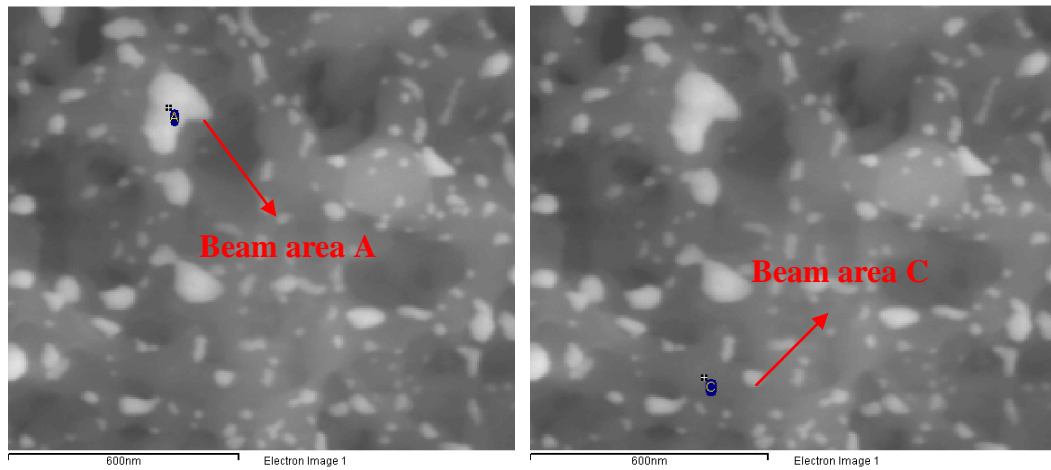


Figure 3.4. A diagram showing the indication of beam area injection by EDX for silica soot layer pre-sintered at 950°C after solution doping.

Table 3.1 Composition of elements in silica soot layer of pre-sintering temperature 950°C after solution doping for beam area A and C.

Elements	Composition, at%	
	Beam area A	Beam area C
C K	6.46	–
O K	68.39	69.16
Si K	11.89	25.79
P K	–	0.99
Cl K	0.47	0.38
Ge L	1.15	2.20
Er M	1.15	1.48
AuM	10.48	-

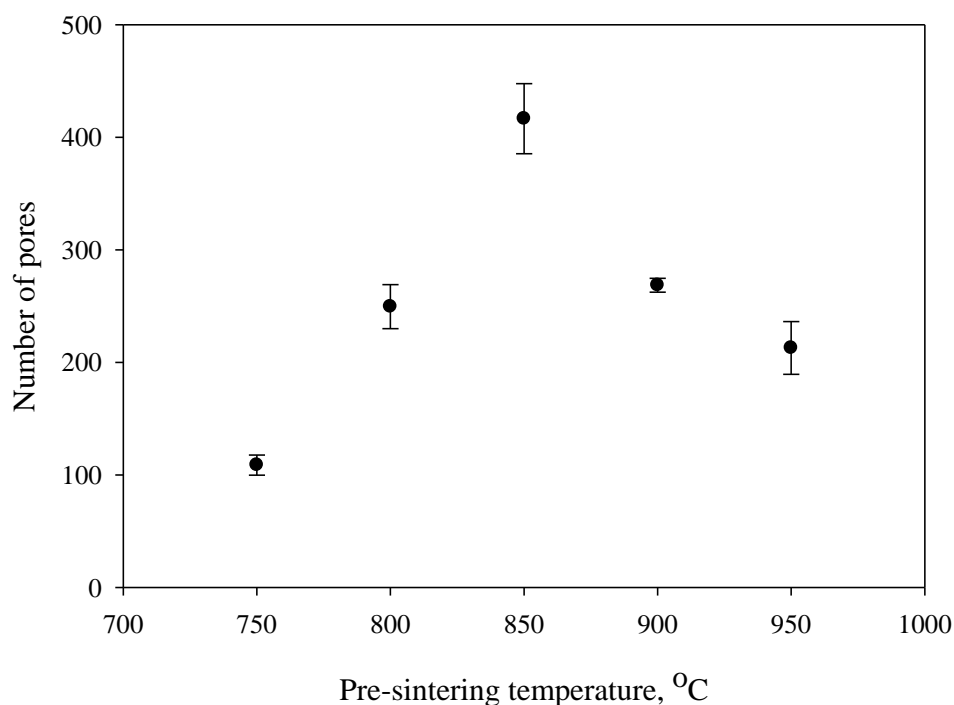


Figure 3.5 Graph for number pores per square area in silica porous soot layer with different pre-sintering temperature.

Number of pores per square area in the silica soot layer varied in different pre-sintering temperature as show in the Figure 3.5. The number of pores per square area was calculated by using images J which is an image processing software. According to Denis Guilhot, number of pores per square area contribute to the amount of erbium ion to be incorporated [4]. The structure of pores allows solution to diffuse into porous silica layer leading to interstitial erbium ion doping into silica layer during the immersed ion in the solution. In conclusion, the high number of pores per square area in silica layer results the high erbium ion concentration incorporation in silica layer. However, we still had the others variation to effect the erbium ion incorporation in silica layer. Hence, we need to find the optimum pre-sintering temperature for a great doping in core layer. The FESEM images in Figure 3.2 show the change in morphology of silica soot layer in different temperature between 750°C to 950°C by varied 50°C. Thus number of pores per square area in silica layer also varies. A peak shows in the graph of number of pores per square area versus pre-sintering temperature. 850°C is an optimum temperature to incorporate the most erbium ion in silica layer. The graph



indicates number of pores per square area in 750°C is about 109 while about 212 number of pores per square area for 950°C. During the FHD process, the particles form a tenuous network containing pores. They adhere together through molecular force. The skeleton of the glass matrix is formed by sintering the particles of the layer together, by heating of the sample. When the pre-sintering temperature is low i.e 750°C, the fine network formation and the particles size seems smaller in resulting the number of pores per square area is low. As the pre-sintering temperature gradually increase, the network formation become strong; the pores become clearer and then increasing in numbers of pores per square area. This induces an increase in particles size and pore size as the pores agglomerate. If the pre-sintering temperature is too high, the partial fusing of silica layer increased and then the number of pores per square area will decrease again as show in 950°C. The pores also become more spherical due to material transfer between the particles. These pores then out-diffuse during the final step of the consolidation process, leading to a fully dense glass layer.

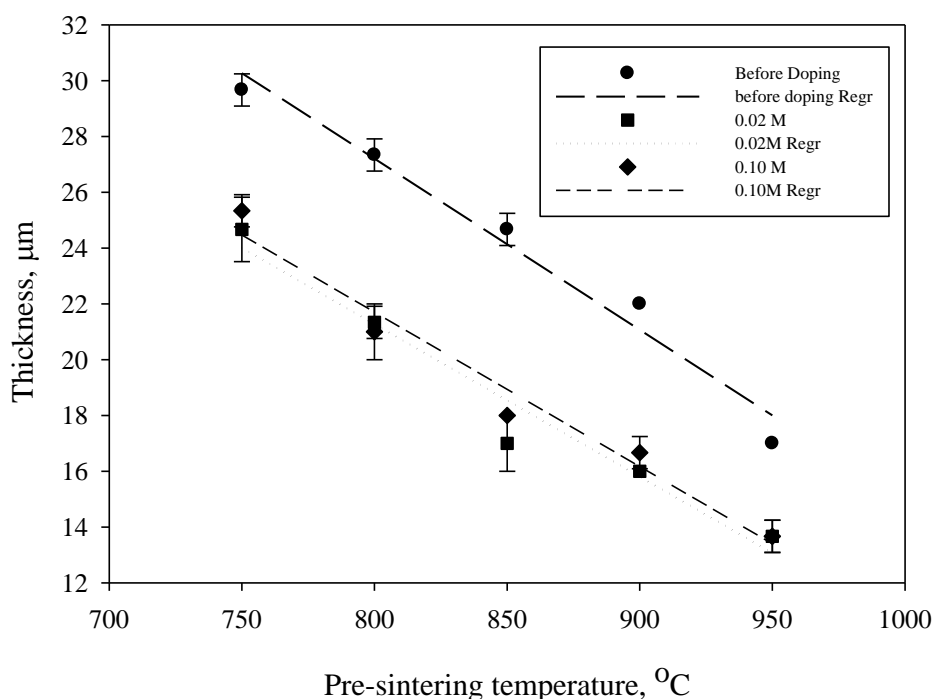


Figure 3.6 Graph shows that the thickness of soot layers varies in different temperature.

The thickness of soot layer had been investigated in different temperatures. The images for thickness of soot layer had been captured by optical microscope and then measured by image J. Magnification 10x had been used in the optical microscope. The gradual increasing in pre-sintering temperature leads to decrease thickness of silica porous soot layer illustrate in Figure 3.6. As shown in Figure 3.6, comparison of thickness of silica soot layer before solution doping and after solution shows that the latter has undergone a decrease of 4-6  $\mu\text{m}$  in thickness. The thickness before solution doping gradually decrease from 30  $\mu\text{m}$  to 17  $\mu\text{m}$  while the thickness for after solution doping in 0.1M and 0.02M erbium chloride ( $\text{ErCl}_3 \cdot 6\text{H}_2\text{O}$ ) decrease from 25  $\mu\text{m}$  to 13  $\mu\text{m}$  respectively. There is no significant difference for the thickness of silica soot layer between the sample with 0.1M and 0.02M erbium chloride ( $\text{ErCl}_3 \cdot 6\text{H}_2\text{O}$ ) solution doping. The silica porous soot layer thickness is an important parameter to optimize the soaking time in the solution. An accurate soaking time can be define by the thickness of silica layer [16]. This will be a cost saving for fabrication in industry. In addition, thickness of silica layer can determine the amount of erbium ion incorporation. As temperature increases, thickness of layer drops due to silica layer that becomes denser [4, 16]. The diffusion erbium ion from solution to silica layer decrease as a result erbium ion concentration incorporation is low.

### **3.6 Non-selective area doping**

For the experiments described in this Section, the dipping time was set to 1 hour [4]. 0.1M erbium chloride ( $\text{ErCl}_3 \cdot 6\text{H}_2\text{O}$ ) in aqueous solution was used. Following solution doping, the samples were consolidated at 1320°C in a tube furnace. The surfaces of the resulting samples were rough and whitish. No fringes were reflected on the surface of samples. A phenomenon always occurs in glass layer called devitrification is suspected to happen in silica layer. Devitrification is a condition where

whitish scum appears on the top surface of glass when the glass remains at high temperature for a long period. Devitrification happens due to high doping in erbium ion concentration. This phenomenon can be overcome by co-doping with aluminium. Figure 3.7 illustrates the images of 0.1M erbium chloride doped samples in different pre-sintering temperature and consolidated at 1320°C.

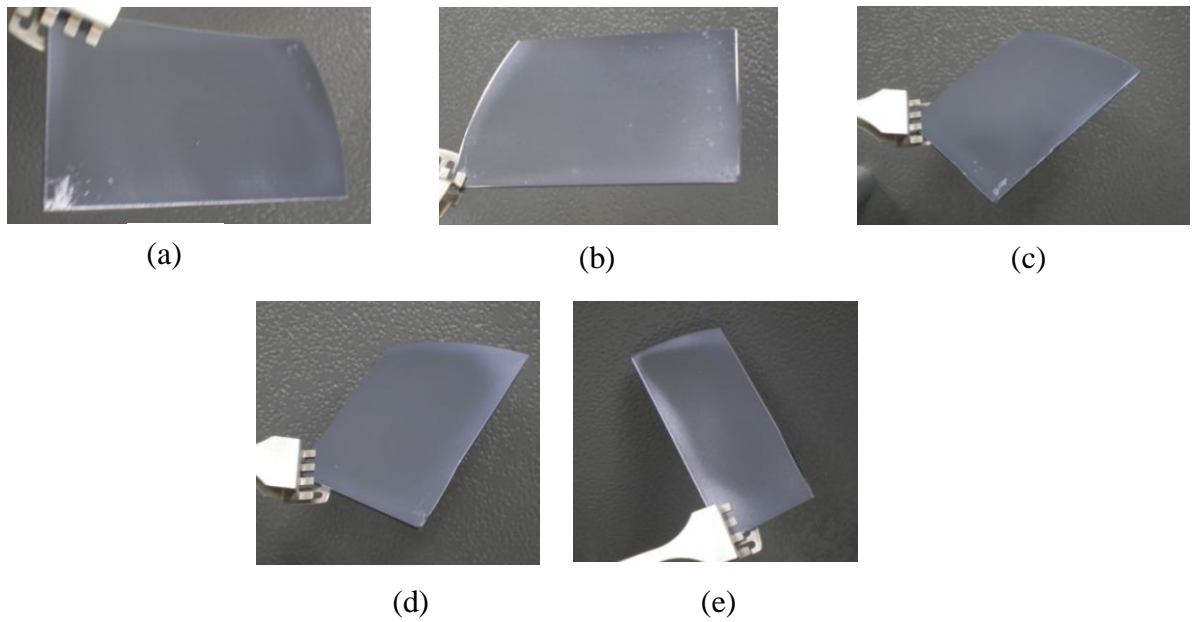


Figure 3.7 The pictures of 0.1M erbium chloride doped samples in different pre-sintering temperature and consolidated in 1320°C.

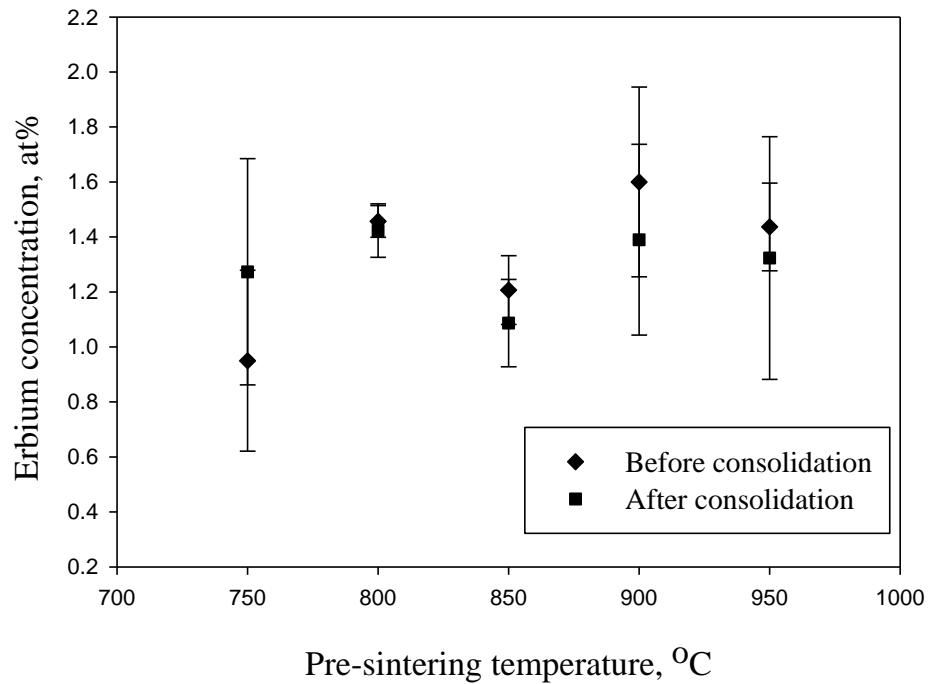


Figure 3.8 Erbium concentration, at% for different pre-sintering temperatures in 0.1M erbium chloride ( $\text{ErCl}_3 \cdot 6\text{H}_2\text{O}$ ) before and after consolidation at  $1320^\circ\text{C}$ .

The erbium ion concentration levels in the silica layer before and after consolidation were investigated. Figure 3.8 shows the results examined by energy dispersive X-ray (EDX). There is no a significant trend of erbium ion concentration incorporated in the different pre-sintering temperature. This proves that the pre-sintering temperature is not a major parameter to affect the erbium ion incorporation into silica layer. There are a few variations such as thickness and number of pores per square area in silica soot layer that affects the erbium ion concentration. According to results from the calculation of pores number, the pre-sintering temperature  $850^\circ\text{C}$  is an optimum temperature. So that erbium ion incorporation in silica layer is the highest concentration among of them. The error bars in Figure 3.8 imply that it is difficult to accurately quantify the erbium ion concentration using this approach. Additionally, there are also two major parameters to consider, number of pores per square area and thickness. However, the erbium ion incorporation into silica layer before and after

consolidation shows that the latter. Temperature at 750°C is the exception among the pre-sintering temperature. The evaporation of dopants in high temperature during consolidation process leads to low erbium ion concentration incorporation.

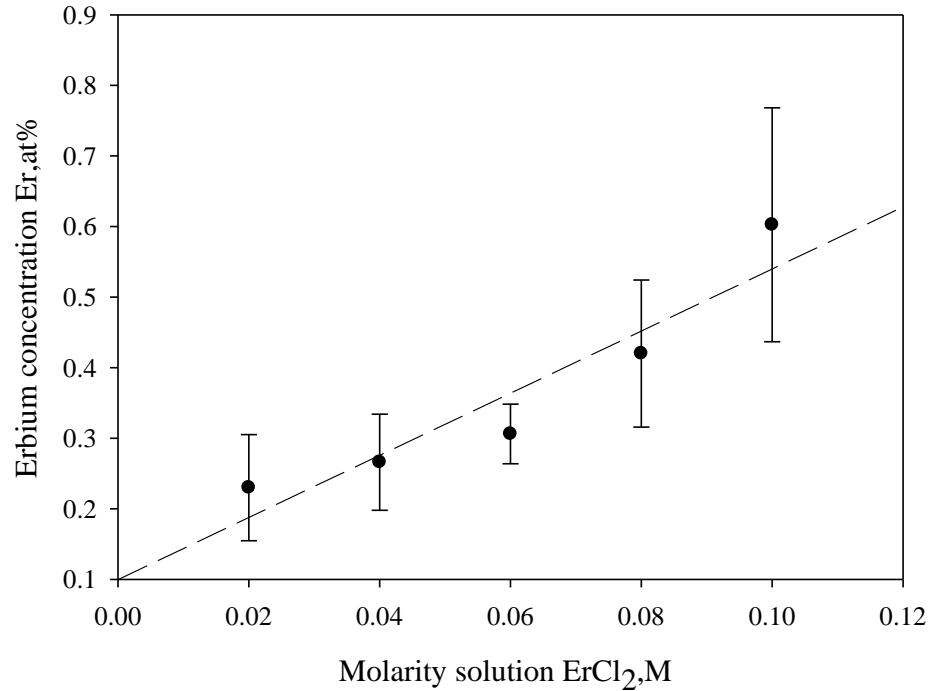


Figure 3.9. Variation of  $\text{Er}^{3+}$  concentration with change in molarity of solution  $\text{ErCl}_3 \cdot 6\text{H}_2\text{O}$  aqueous.

A more detailed description about the influence of the erbium ion concentration incorporated in silica layer by strength of solution is shown in Figure 3.9. The graph shows erbium concentration incorporated into soot layer for 1 hour where the pre-sintering temperature is 850°C and then consolidated in 1320°C. In theory, the higher strength of solution results the higher erbium ion concentration incorporated into silica layer [4]. Experiment results shows that an increasing in ion  $\text{Er}^{3+}$  concentration incorporation with the strength of solution, i.e. molarity. In Figure 3.9, the variation in molarity corresponded to ion  $\text{Er}^{3+}$  concentration increase from 0.22 at% to 0.60 at%. As strength of solution increase, molarity change from 0.02M to 0.10M in same number of ion  $\text{Er}^{3+}$  in solution increase. In resulting incorporation of ion  $\text{Er}^{3+}$  into porous silica soot layer will increase with formation of  $\text{SiO}_2\text{-Er}_2\text{O}_3$  in silica network during

consolidated [15, 18]. Thus the erbium ion embeds in silica network increase in the molarity of solution. The 0.02M sample displayed no whitish particles and contains fringes. However, the fringes still appear in 0.04M and 0.06M samples. For 0.08M samples, the fringes cannot be observed but still have a clear surface. For the high molarity, 0.10M samples, the white particles distribute and cover the consolidated surface and fringes disappear in the samples. The phenomena is likely due to crystallization of cristobalite and silimanite crystallize in the layer called devitrification [4]. It is proven in the pre-sintering temperature samples doped with 0.1M erbium chloride solution. The images in Figure 3.10 reveal whitish particles distribution increase in edge of the samples as the molarity of solution increase.

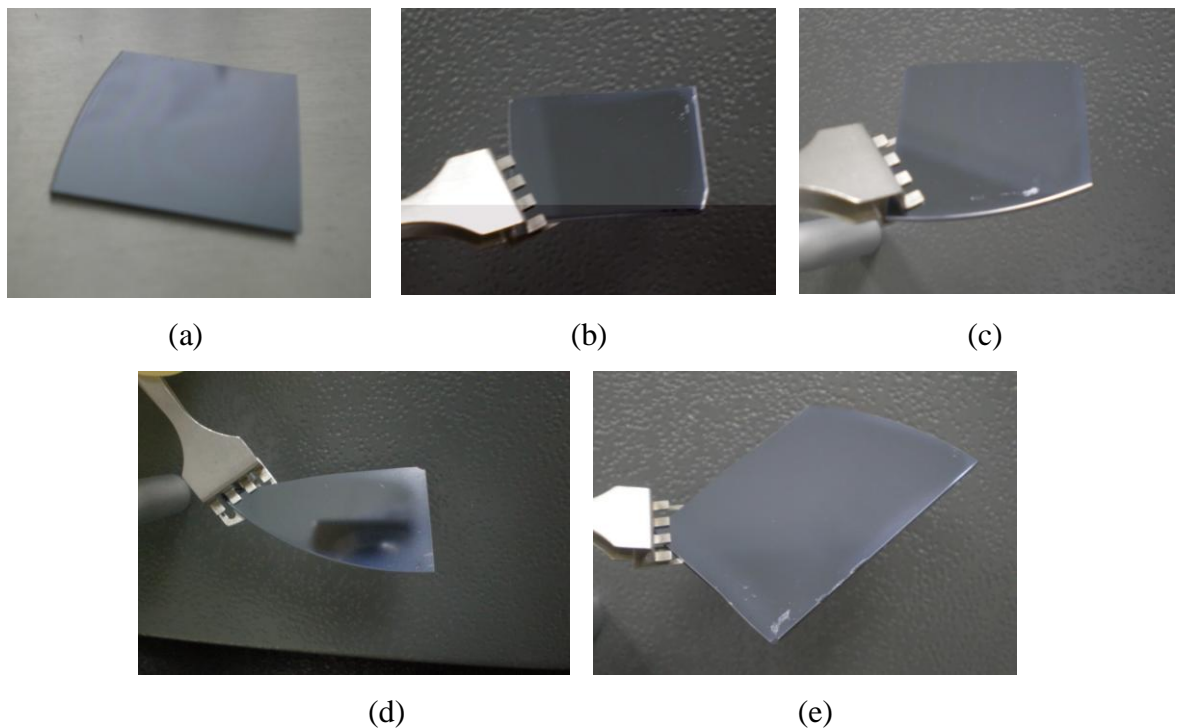


Figure 3.10. Images show the changes in molarity of erbium chloride ( $\text{ErCl}_3 \cdot 6\text{H}_2\text{O}$ ) solution doping in silica layer after consolidation  $1320^\circ\text{C}$ . (a) 0.02M (b) 0.04M (c) 0.06M (d) 0.08M (e) 0.1M

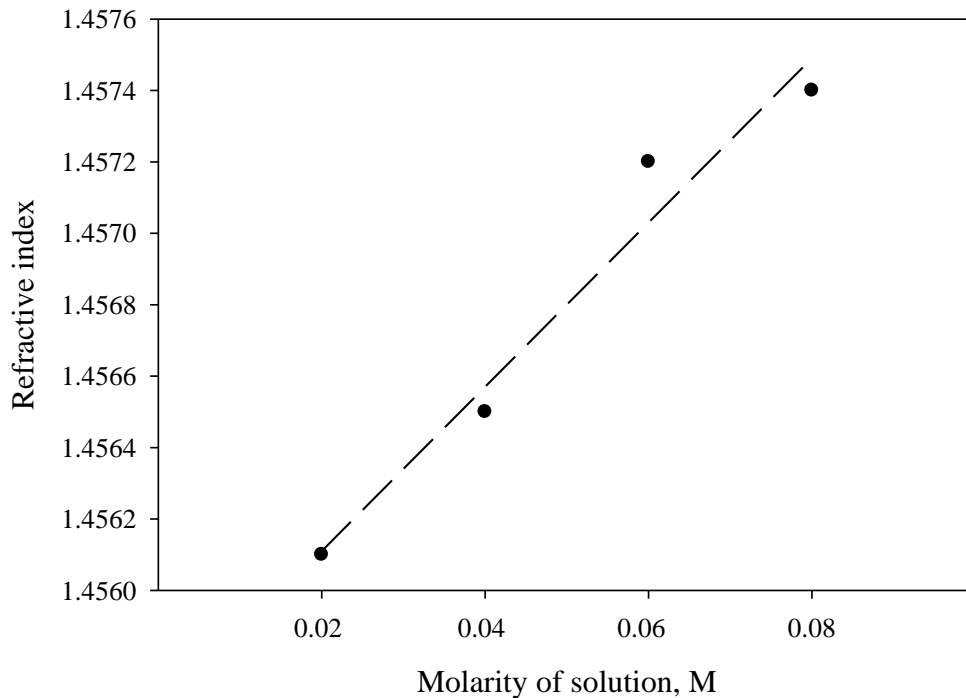


Figure 3.11. Refractive index of Erbium doped silica layer as a function of molarity of solution

The refractive index of layers was measured by using prism couple. The erbium ion concentration increases with the strength of solution in results the refractive index increase. Figure 3.11 shows the changes of refractive index at wavelength 1550 nm as a function of molarity in ion  $\text{Er}^{3+}$  solution. An increasing trend happened in refractive index which as same as the trend in erbium ion concentration with strength of solution which mention above. As the addition of ions with large radius such as  $\text{Er}^{3+}$  makes the dipole strength of non-bridging oxygen increase and hence refractive index increase [9]. The refractive index changes from 1.4561 to 1.4574 for 0.02M and 0.08M of solution strength samples. The difference between two solutions strength was about 0.0893%. We could not measure the refractive index for 0.1M sample due to the surface of sample was too rough.

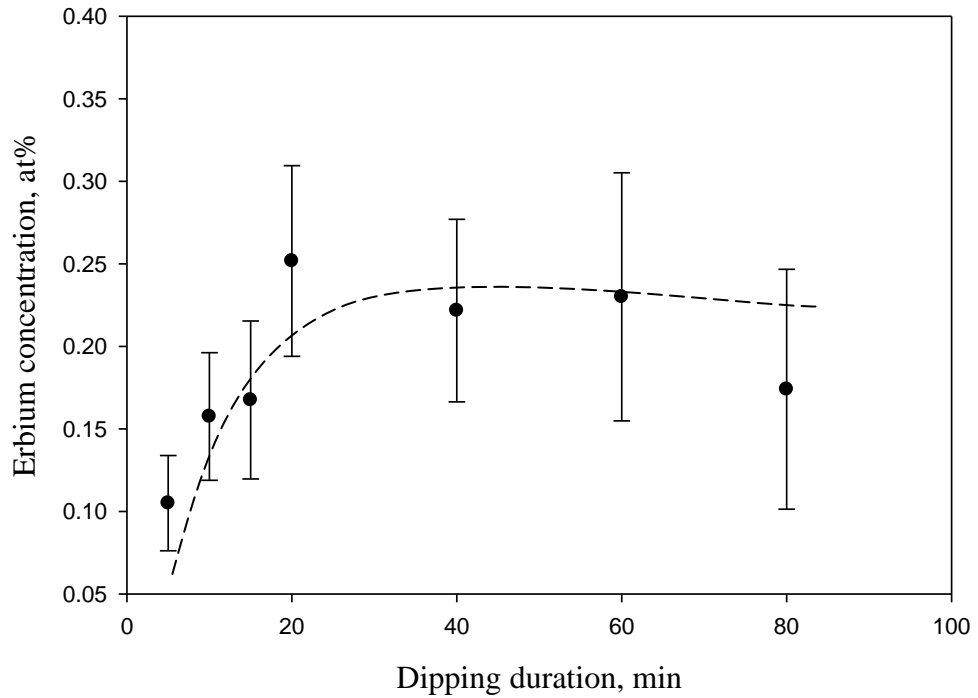


Figure 3.12. Concentration ion  $\text{Er}^{3+}$  incorporated dependence dipping duration.

The dipping duration is another parameter in solution doping. The dipping duration was set as 1 hour as a standard in solution doping. There is the purpose to manage a saturation point in case can reduce the dipping duration of samples from 1 hour to lower time. The dipping duration samples were varied from 5 to 80 minutes when doping in 0.02M erbium chloride ( $\text{ErCl}_3 \cdot 6\text{H}_2\text{O}$ ) solution. Figure 3.12 shows  $\text{Er}^{3+}$  ion concentration varies in dipping duration is an increase trend in 20 minutes and saturated after 20 minutes in dipping duration. We assume there is a saturation trend after 20 minutes because the mean value is 0.23 at% with standard deviation of 0.02, which is considered large. As such, we believe that the trend shown points to saturation effects. Thus the investigation helps to obtain an optimized dipping duration of 20 minutes for porous silica layer in pre-sintering temperature in  $850^\circ\text{C}$  with  $18 \mu\text{m}$  in thickness.



### 3.7 Summary

In this chapter, the solution doping of planar waveguide has been described. The rare-earth ion incorporation method has been roughly explained in the first section. The principle of solution doping was also illustrated. The effect of pre-sintering temperature to soot layer has been investigated in various parameters such as thickness and number of pores per square area. Subsequently the erbium ion concentration in silica layer has been studied by measuring using EDX. The parameter such as strength of solution and dipping duration were used to vary the erbium ion concentration incorporated.

#### References:

- [1] Y. Hibino, T. Kitagawa, M. Shimizu, F. Hanawa, and A. Sugita, "Neodymium-doped silica optical waveguide laser on silicon substrate," *Photonics Technology Letters, IEEE*, vol **1**, pp.349, 1989.
- [2] F. Z. Tang, P. McNamara, G. W. Barton, and S. P. Ringer, "Multiple solution-doping in optical fibre fabrication I - Aluminium doping," *Journal of Non-Crystalline Solids*, vol **354**, pp.927, 2008.
- [3] F. Z. Tang, P. McNamara, G. W. Barton, and S. P. Ringer, "Multiple solution-doping in optical fibre fabrication II - Rare-earth and aluminium co-doping," *Journal of Non-Crystalline Solids*, vol **354**, pp.1582, 2008.
- [4] D. A. Guilhot, in *Faculty of Engineering, Science and Mathematics, Optoelectronics Research Centre (University of Southampton, 2004)*, p. 165pp
- [5] J. Bonar, J. A. Bebbington, J. S. Aitchison, G. D. Maxwell, and B. J. Ainslie, "Aerosol doped Nd planar silica waveguide laser," *Electronics Letters*, vol **31**, pp.99, 1995.
- [6] J.R.Bonar, M.V.D.Vermelho, P.V.S.Marques, A.J.McLaughlin, and J.S.Aitchison, "Fluorescence lifetime measurement of aerosol doped erbium in phosphosilicate planar waveguides," *Optics Communications*, vol **149**, pp.27, 1998.
- [7] A. V. Belov, E. M. Dianov, G. G. Devy'atykh, V. F. Khopin, A. N. Gur'yanov, and Y. B. Zverev, "Erbium-Doped Fibers Based on Cesium-Silicate Glasses," *Optical Fiber Technology*, vol **6**, pp.61, 2000.
- [8] J. R. Bonar, J. A. Bebbington, J. S. Aitchison, G. D. A. M. G. D. Maxwell, and B. J. A. A. B. J. Ainslie, "Low threshold Nd-doped silica planar waveguide laser," *Electronics Letters*, vol **30**, pp.229, 1994.
- [9] S. I. Ro, Y. S. Jung, and D. W. Shin, "The effects of Er/Al co-doping on the fluorescence of silica waveguide film," *Journal of Ceramic Processing Research*, vol **2**, pp.155, 2001.
- [10] D. A. Guilhot, in *Science and Mathematics, Optoelectronics Research Centre (University of Southampton, 2004)*, p. 165pp
- [11] J. E. Townsend, in *Electronics and Computer Science (University of Southampton, 1990)*.

- [12] F. Z. Tang, P. McNamara, G. W. Barton, and S. P. Ringer, "Nanoscale characterization of silica soots and aluminium solution doping in optical fibre fabrication," *Journal of Non-Crystalline Solids*, vol **352**, pp.3799, 2006.
- [13] A. Dhar, M. C. Paul, M. Pal, A. K. Mondal, S. Sen, H. S. Maiti, and R. Sen, "Characterization of porous core layer for controlling rare earth incorporation in optical fiber," *Opt. Express* vol **14**, pp.9006, 2006.
- [14] B. Gonzalez-Diaz, B. Diaz-Herrera, R. Guerrero-Lemus, J. Mendez-Ramos, V. D. Rodriguez, C. Hernandez-Rodriguez, and J. M. Martinez-Duart, "Erbium doped stain etched porous silicon," *Materials Science and Engineering: B*, vol **146**, pp.171, 2008.
- [15] J. E. Townsend, S. B. Poole, and D. N. Payne, "Solution-doping technique for fabrication of rare-earth-doped optical fibres," *Electronics Letters*, vol **23**, pp.329, 1987.
- [16] A. Dhar, M. C. Paul, M. Pal, A. K. Mondal, S. Sen, H. S. Maiti, and R. Sen, "Characterization of porous core layer for controlling rare earth incorporation in optical fiber," *Opt. Express*, vol **14**, pp.9006, 2006.
- [17] F. Z. Tang, P. McNamara, G. W. barton, and S. P. Ringer, "Microscale Inhomogeneities in Aluminium Solution doping of silica based optical fibers," *Journal of American Ceramic Society*, vol **90**, pp.23, 2007.
- [18] A. Dhar, M. C. Paul, M. Pal, S. K. Bhadra, H. S. Maiti, and R. Sen, "An improved method of controlling rare earth incorporation in optical fiber," *Optics Communications*, vol **277**, pp.329, 2007.

## **Chapter 4 Selective area doping**

### **4.1 Introduction to selective area doping**

Rare-earth ions incorporated into silica layer have been studied in Chapter 3. Solution doping was chosen in our work for erbium ion incorporated into porous germano-silicate layer. It had been used for optical amplifiers and fiber laser [1-4]. As the demand for high-bandwidth applications in the home increases, so does the demand for suitable optical amplifiers to meet metropolitan-area-network and local-area-network. Suitable devices must minimize power and size requirement. The EDWA offers a great promise in integration of many functions onto an easily mass-produced photonic integrated circuit. EDWAs are attractive as they minimize the size of devices while maintaining amplification.

The solution doping method offers flexibility in doping rare earths in various concentrations. However, controlling of rare-earth concentration in a certain area of integrated circuit and the uniformity of doping are still major problems in this process. In this case, erbium ions only need to incorporate into amplifying waveguide for EDWA serves as amplifier to the optical signal. The incorporation of erbium ion will be excluding for passive waveguide such as laser pump or wavelength division multiplexer. For instance, the embedded of erbium ion in laser pump will cause the absorption of optical signal to occur. This will reduce pump efficiency levels. Thus net gain of amplifier in EDWA decreases due to reduction of pump efficiency..

### **4.2 Review of selective area doping**

There are two approaches in integrated optics, namely monolithic and hybrid integration. The hybrid approach involves the growth of optically active materials such as

III-V semiconductors, polymers and silicon on a substrate surface. There are several advantages for using semiconductor compound in integrated circuit. This is because of semiconductor compound contains high speed, wide range of bandgaps available for optical signal processing and also the possibilities of high temperatures operation. Selective area doping was applied in hybrid integration [5]. Ion implantation is an attractive and useful method where provide ion bombardment as a processing tool for selective area doping [6]. The advantage offers by ion implantation over other doping approaches include an excellent control of depth profile and concentration of dopants. However, effects of ion beam produced lattice defects is a main problem occur in ion implantation method.

Recently, the research attention moves towards monolithic integration. For instance, EDWA is a good example to use selective area doping as showed in above section. In our study, flame hydrolysis deposition (FHD) was used to deposit silica porous layer followed by aqueous solution doping. Liquid phase is applied in selective area doping. Selective area doping is an analog rare-earth incorporation method of solution doping. The selective area doping involved two majors steps same as solution doping. They are deposition of porous silica layer comprising refractive index raising materials like germanium or phosphorus at high temperature by flame hydrolysis deposition (FHD). The following step is dripping the rare-earth containing aqueous solution by using syringe or pipette in specific area of porous silica soot layer. In our studies, selective area doping was used to investigate the variation of diameter in doping area, erbium ion concentration and distribution of concentration.

#### **4.3 Selective area doping set up (Experimental method).**

Having demonstrated the basic technique in rare earth doping of planar silica layers, our next step was to dope only specific areas within the sample. The objective here is to

facilitate monolithic integration of passive and active devices onto a single chip. As the first proof-of-principle, we chose the technique that is the easiest to adopt. Instead of immersion, the pre-sintered sample was doped by applying rare-earth salt solution droplets using a syringe or pipette, as shown schematically in Figure 4.1. A ‘quarter wafer’ was used as it is a more economically option compared to using a full wafer. The porous silica soot layer has rising refractive index dopants such as germanium oxide, phosphorus oxide and boron oxide in pre-sintering temperature 850°C.

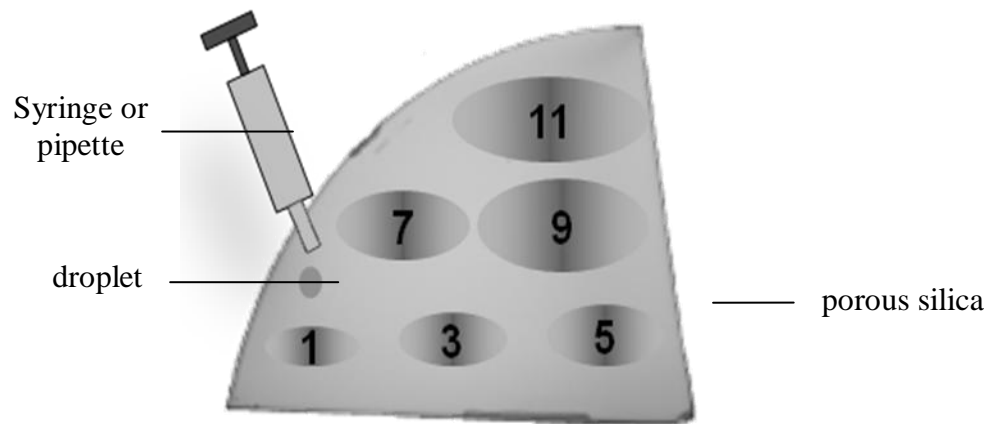


Figure 4.1 Selective area doping using a syringe (number indicating number of droplets applied).

A 0.1M solution of  $\text{Er}^{3+}$  was prepared by dissolving high purity erbium chloride ( $\text{ErCl}_3 \cdot 6\text{H}_2\text{O}$ ) in deionized water. A syringe or pipette was used to suck the solution and drip in silica porous layer. The volume of droplets could be varied in pipette. Each droplet contains ~1ml of erbium solution for syringe, and follows a circular diffusion profile. This diffusion area increases with the number of droplets applied. The samples were dried in room temperature for 30 minute then followed by drying in oven for 30 minute. The doped regions display good surface morphology, with no signs of cracks or bubbles. The samples were then fully consolidated in 1320°C. Following the consolidation, we performed EDX

measurements to confirm the presence of erbium in the doped regions. The samples were found to contain no surface defects.

#### **4.4 Selective area by syringe**

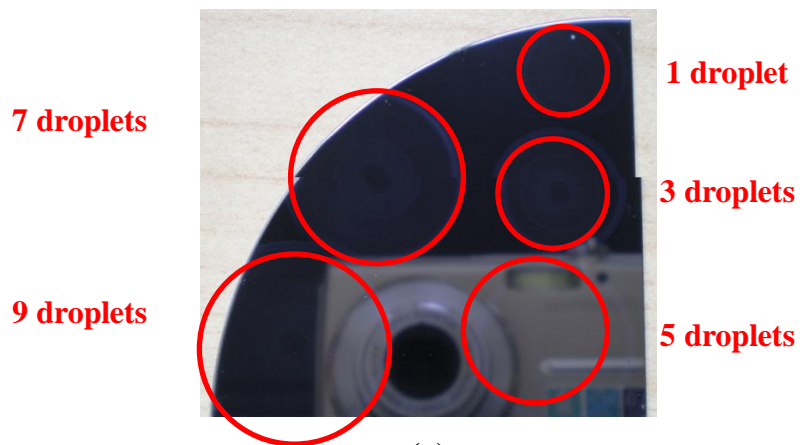
A syringe was used in this experiment. The experimental method is similar to that described in chapter 3. A porous silica soot layer was deposited on silicon substrate following 0.1M erbium chloride ( $\text{ErCl}_3 \cdot 6\text{H}_2\text{O}$ ) aqueous solution was prepared and dripped by using a syringe. One droplet was dripped into porous silica soot layer following the drying method as mention above. The drying condition was defined by using bare eye where the soot layers turn in origin colour. It takes about 30 seconds for every droplet. Subsequently, another droplet of salt solution was dripped into porous silica soot layer. This method is called multiple cycles in selective area doping. Droplets were continuously dripped without drying up the soot layer called one cycle. The variation of diameter of doping area and erbium ion concentration in number of droplets had been investigated in one and multiple cycles. The volume of each droplet was also defined by bare eye. Accurate controlling droplet volume is a major issue for this method.

##### **4.4.1 Diameter of selective doping area**

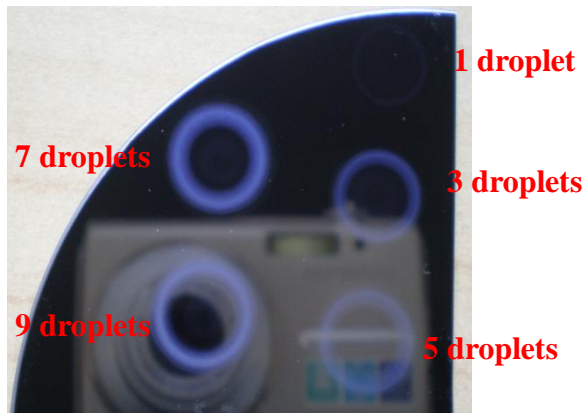
A variation of diameter of circle versus number of droplets was investigated. Figure 4.2 illustrates those consolidated samples dripped with 0.1M erbium chloride in one and multiple cycles by using syringe. The numbers of droplets were varied from 1 to 9 drops. Comparing the two pictures in one and multiple cycles dripping, shows that controlling the diameter of circle can be done well by multiple cycles' method. The diameter of circles in one cycle gradually increases with the number of droplets. Diffusion occurs when droplets drip into silica layer. As continuously dripping the droplets, the molecular force in silica

layer increases and puts toward the soot particles to aside. The erbium ion will diffuse and spread into porous silica layer. In results area of doping will spread as continuously dripping erbium droplets into the silica soot layer. This leads to diameter of circles increases with droplets. For multiple cycles, every droplet will go through drying method following the others droplets drip into silica layer. The molecular force cause by water molecule reduces as the silica soot layer dried up. Diffusion spread in a limit area due to molecular force reduces in resulting the diameter of circles was controlled in certain size.

In addition to this, there exists ring-like formation following consolidation. Ring-like formation occur because cumulative of erbium ions in silica layer when the droplets continuously dripped. The molecule force increases as continuously dripped, and then push the erbium ion aside. A ring-like form will be existed following by dried up process. The appearance of rings became clearer and thick as the droplets increased for multiple cycles. For one cycle samples, the rings were not as clear as multiple cycle samples. There are no fringes in the selective area doping results by high strength of erbium ion solution. Devitrification occurs in high strength of solution. This is proven in related section of chapter 3. Figure 4.3 shows that failed samples of selective area doping. There are some problems occurs by using syringe. The volume of every droplet can not control as well as by using syringe leads to different size of rings appeared as drip in a few droplets. The Figure 4.3 (a) shows the problem occurred in controlling volume by using syringe. Figure 4.3 (b) shows that the over flow of doping area occurred in one cycle method. Continuously dripping will cause the doping solution diffuse to other doping area. Controlling in erbium ion concentration incorporated is not in high accurate due to over flow of doping area.

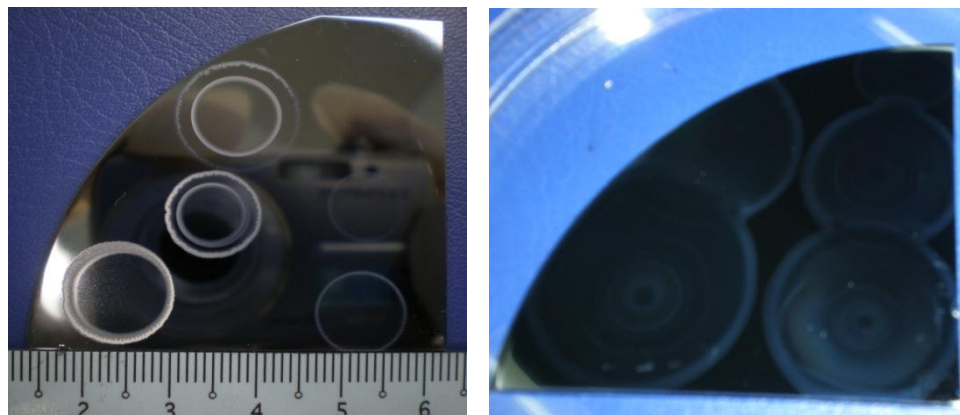


(a)



(b)

Figure 4.2 Pictures of selective area doped with 0.1M erbium chloride ( $\text{ErCl}_3 \cdot 6\text{H}_2\text{O}$ ) in pre-sintering temperature  $850^\circ\text{C}$  of silica soot layer by using syringe (a) one cycle (b) multiple cycles



(a)

(b)

Figure 4.3 Pictures of failed samples in selective area doped with 0.1M erbium chloride ( $\text{ErCl}_3 \cdot 6\text{H}_2\text{O}$ ) in pre-sintering temperature  $850^\circ\text{C}$  of silica soot layer by using syringe (a) one cycle (b) multiple cycles



The diameter of circles and rings width in one and multiple cycles were measured by image J. Figure 4.4 and 4.5 show the graph of circle diameter and ring width in one cycle. An increasing trend in diameter of circle with droplets shows in the graph. As mention above, the molecular force increase due to continuously dripping leads diffusion in doping area spread. The diameter of circle also increases with droplets. The diameter of circle increases ~ 86% in change 1 to 9 droplets. It is a huge increasing in change of diameter circle from 12.431mm to 23.15mm in varied 1 to 9 droplets. The measured figure of diameter in circle and ring shows in table 4.1. A different trend is showed in ring width. An increasing trend shows from 1 to 5 droplets and decreases from 5 to 9 droplets. It increases from 0.703 mm to 1.126 mm then slightly decreases to 1.036mm. Ring width does not affect much by the number of droplets. EDX was used to determine elements composition in center towards to ring.

Table 4.1 Diameter of circle and ring width in one cycle

Number of droplets	Diameter of circle, mm $\pm 0.005$	Diameter of ring, mm $\pm 0.005$
1	12.431	0.703
3	15.304	1.084
5	19.199	1.126
7	20.802	1.091
9	23.150	1.036

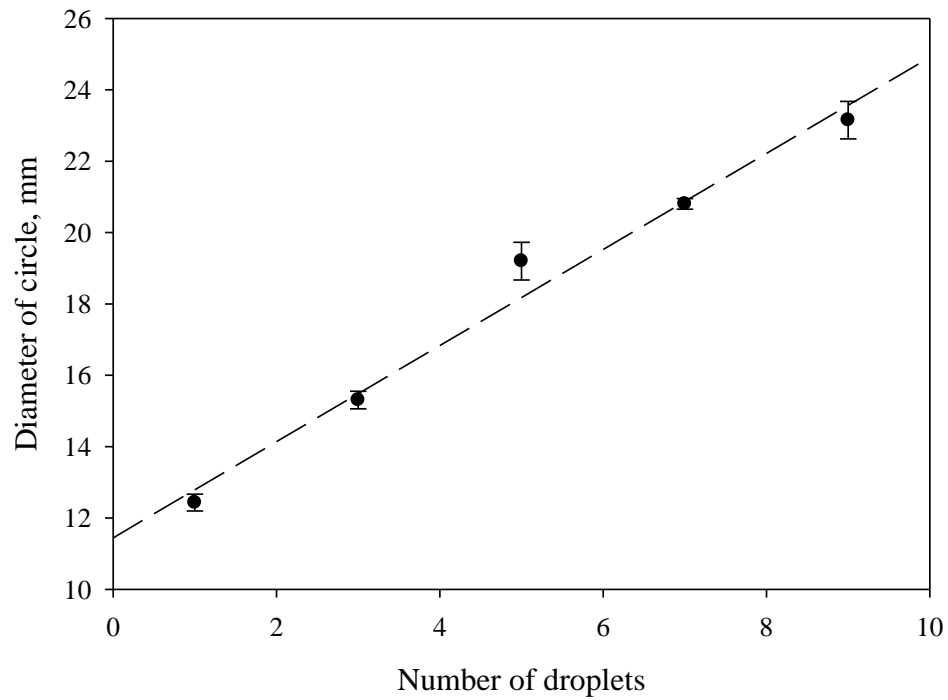


Figure 4.4. Graph of diameter of circle, mm in change of droplets doped with 0.1M erbium chloride ( $\text{ErCl}_3 \cdot 6\text{H}_2\text{O}$ ) by using syringe (one cycle)

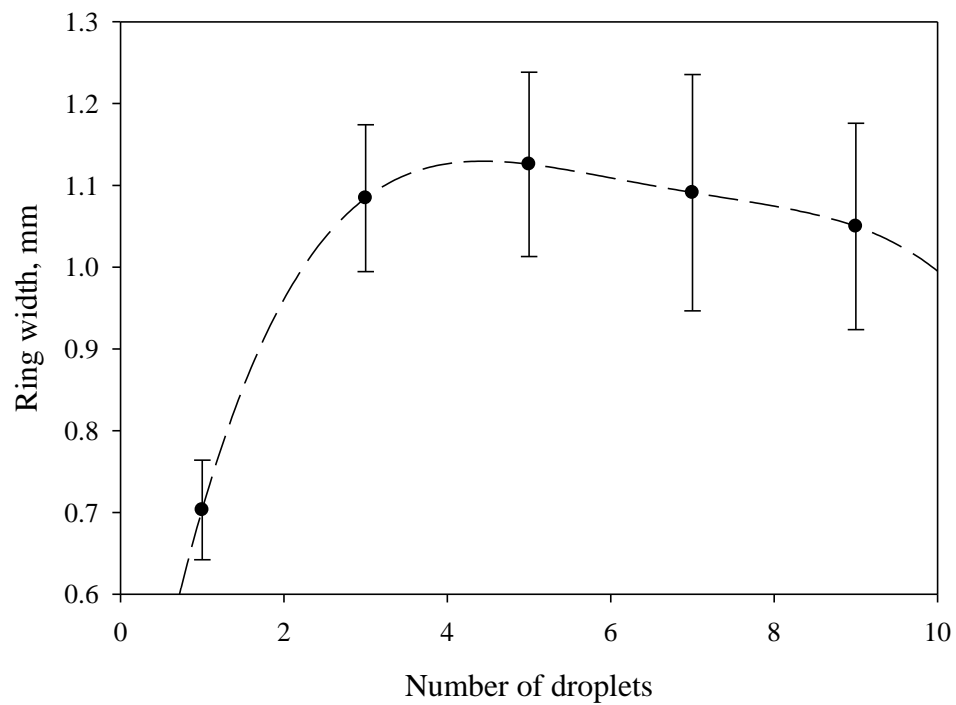


Figure 4.5 Graph showed that ring's width, mm in change of droplets with 0.1M erbium chloride ( $\text{ErCl}_3 \cdot 6\text{H}_2\text{O}$ ) by using syringe (one cycle)

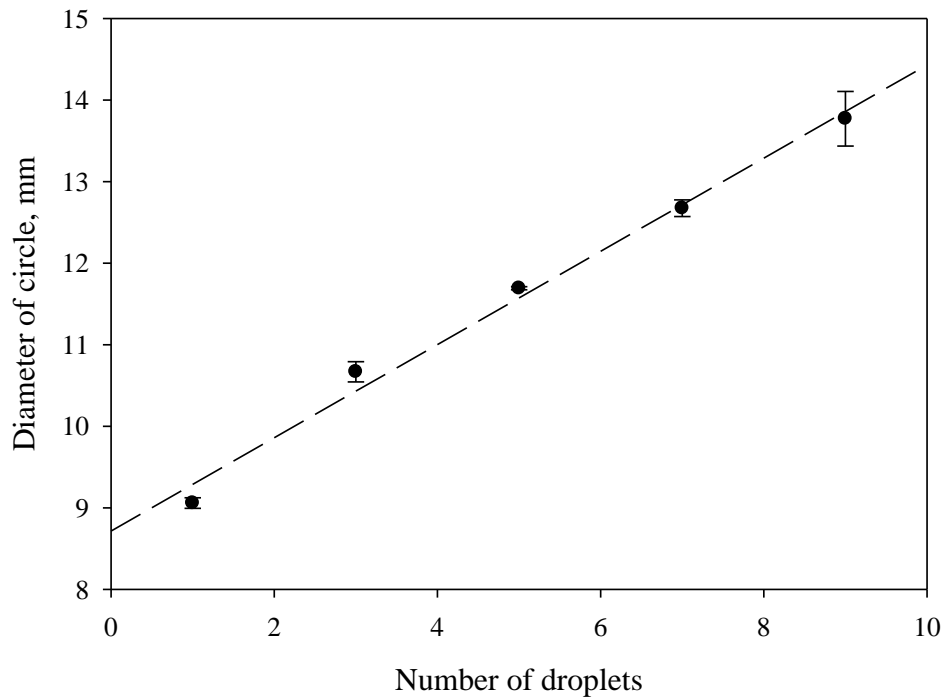


Figure 4.6. Graph showed that diameter of circle, mm in change of droplets with 0.1M erbium chloride ( $\text{ErCl}_3 \cdot 6\text{H}_2\text{O}$ ) by using syringe (multiple cycles)

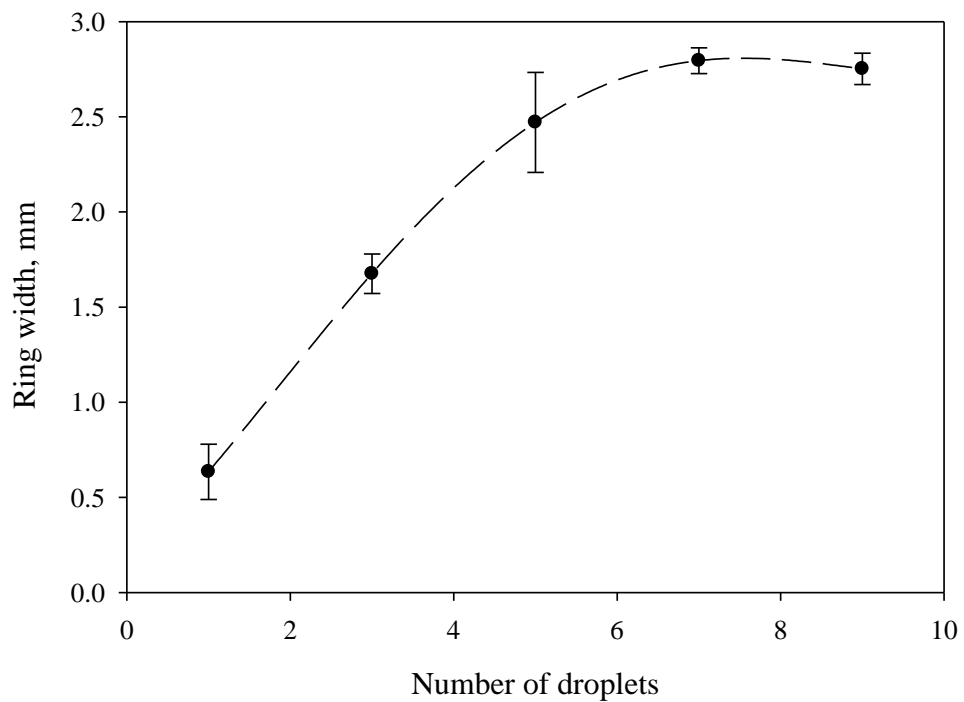


Figure 4.7. Graph showed that ring's width, mm in change of droplets with 0.1M erbium chloride ( $\text{ErCl}_3 \cdot 6\text{H}_2\text{O}$ ) by using syringe (multiple cycles)

Table 4.2 Diameter of circle and ring width in multiple cycles

Number of droplets	Diameter of circle, mm $\pm 0.005$	Diameter of ring, mm $\pm 0.005$
1	9.058	0.634
3	10.667	1.675
5	11.692	2.470
7	12.673	2.795
9	13.077	2.752

Figure 4.6 and 4.7 show that the graph of circle diameter and ring width changed with droplets in multiple cycles. An increasing trend shows in graph of circle diameter as same in one cycle sample. The diameter of circle increases from 9.058 mm to 13.077 mm in between 4.019 mm. It increases ~44% in diameter of circle. Comparing the increase in circle diameter in one cycle with multiple cycles shows that a high increasing trend occurs in one cycle. By the observation during the experiment carried out, the 1<sup>st</sup> drop diameter usually had smaller spread diameter. As the more droplets added to the same circle, the spread of circle diameter would be slightly increased. The spread of circle diameter would be stop after a few droplets were added and a white ring was formed. The white ring served as a barrier to block the spread of diameter. From Figure 4.7, the ring width increases with number of droplets. As shows in picture, the white rings are getting clearer and thicker as same with results in ring width graph. EDX was used to determine the composition in ring of selective area doping.

#### 4.4.2 Erbium ion concentration with number of droplets

Erbium ion concentration increases as the position moves from center towards to ring illustrates in Figure 4.8. The graph of erbium ion concentration incorporation shows the highest concentration in ring position while the center position was the lowest. This is

proven by the appearance of white ring is erbium ion concentration effect. The highest erbium ion concentration will show the most clearest of white ring effect. As droplets increases, erbium ion concentration increases in center and between positions of circle. For the ring position, the erbium ion concentration increases from 3.107 wt% to 4.011 wt% for 1 to 3 droplets and then decreases to 3.34 wt% for 9 droplets. The erbium ion concentration in selective area doping for one cycle is lower than non-selective area doping. In non-selective area doping, erbium ion concentration is around 6 wt% to 12 wt% while the highest of erbium ion concentration achieved ~ 4wt% in selective area for one cycle. The erbium ion concentration in one cycle does not affect much by the number of droplets and position compare to multiple cycles. The diffusion of erbium ion concentration is quite uniform. This is because the erbium ion concentration is not a big change when position of circle move towards.

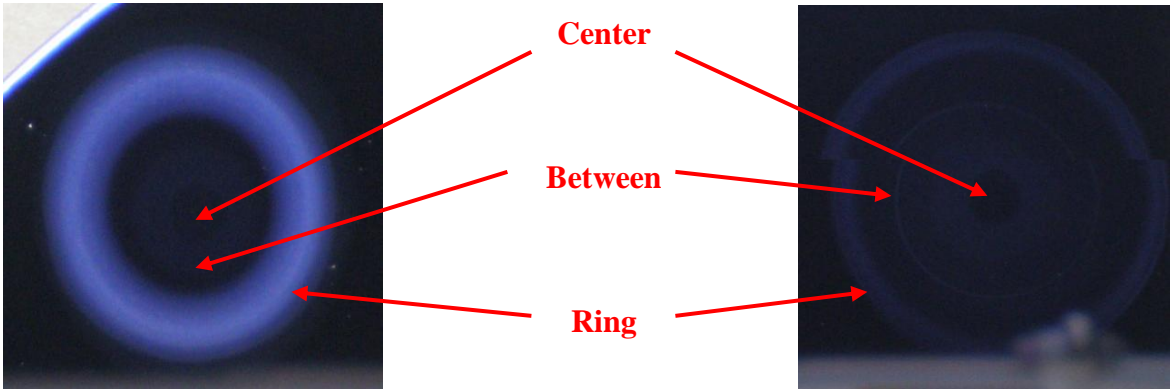


Figure 4.8 Position of circle in selective area doping measured by EDX

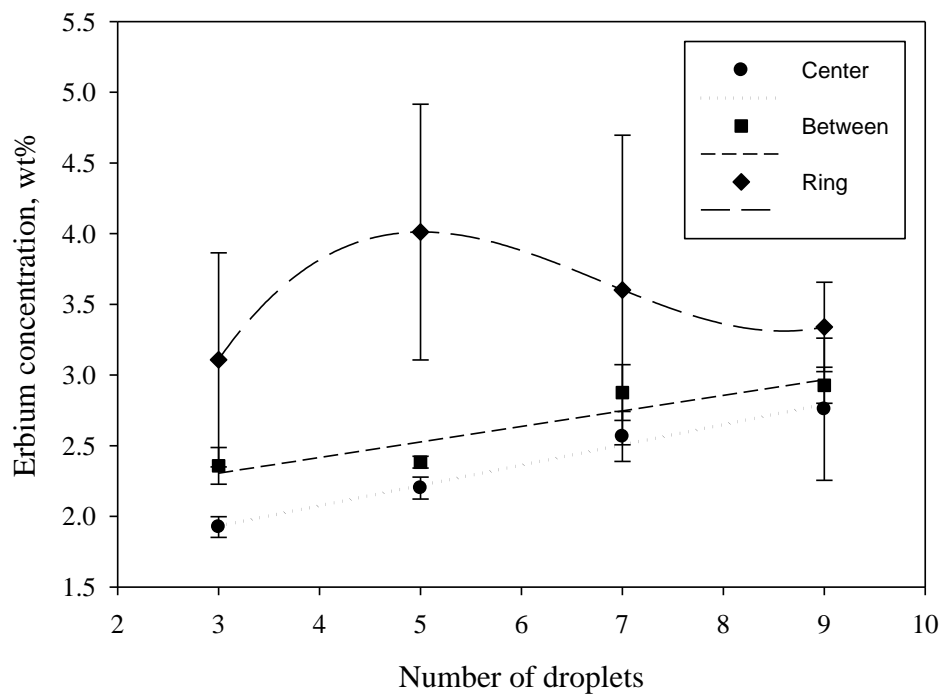


Figure 4.9. Graph showing different position of erbium concentration, wt% with change in number of droplets in 0.1M erbium chloride by using syringe (one cycle)

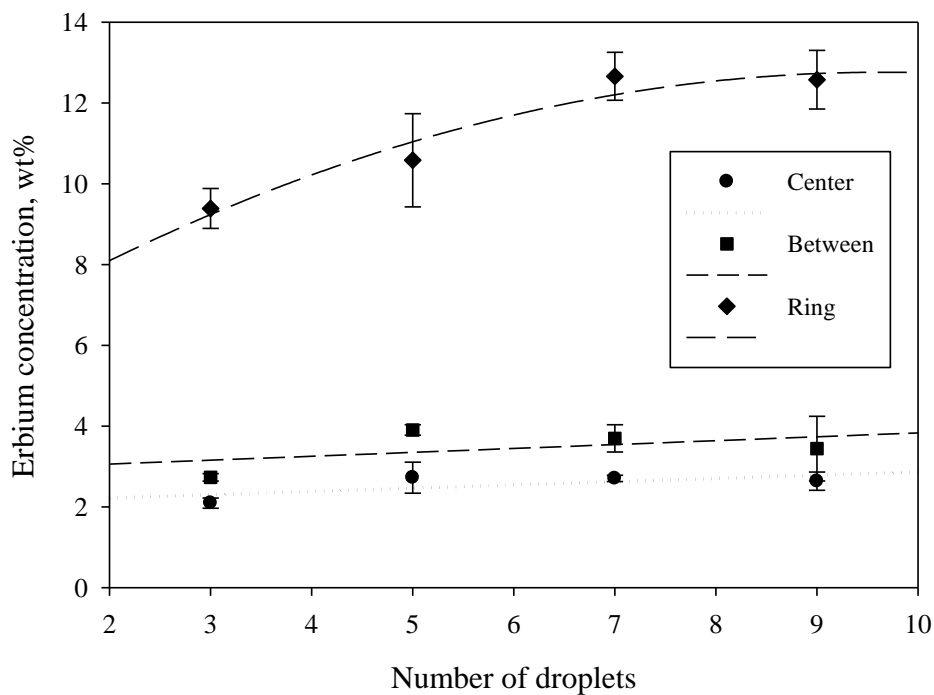


Figure 4.10. Graph showing different position of erbium concentration, wt% with change in number of droplets in 0.1M erbium chloride by using syringe (multiple cycles)

As shown in Figure 4.9, the erbium ion concentration increases when the position moved from center to ring. It shows a similar trend in multiple cycles in Figure 4.10. A large increase of erbium ion concentration in ring position in multiple cycles compares to one cycle. For instance, it varies ~6 wt% from ~3 wt% in one cycle to ~ 9 wt% in multiple cycles for 3 droplets. A high erbium ion concentration incorporated into the ring position that varies from 9.388 wt% to 12.574 wt% as number of droplets increases. The ring serves as a barrier to block the spread of diameter in multiple cycles resulting in high erbium ion concentration that accumulates in the ring position. As the ring width increases, the higher erbium ion concentration is incorporated into silica layer. In conclusion, the trend shows in the ring width is similar to the erbium ion concentration incorporated in the ring as the number of droplets increases. This is proven by the graph as shown in one cycle and multiple cycles.

#### **4.4.3 Distribution of erbium ion concentration**

A line scan was taken 2 mm distance by using EDX. The line scan was taken from middle of ring towards the center indicated distribution of erbium ion concentration in selective area doping. A graph showing the counts collected by sensor in EDX versus the normalized radius represented erbium ion concentration and distance in circle. A fluctuation trend indicated erbium ion concentration is not affect as distance move towards to between positions in one cycle. This implies the uniformity of doping area for 3 droplets. As the droplets were added, the erbium ion concentration slightly increases in ring position in one cycle. The graph in Figure 4.11 is proven this trend and other compositions of elements such as phosphorus and germanium also showed in the graph. Phosphorus and germanium shows the similar trend for 3 and 9 droplets. Phosphorus contains higher counts which mean high concentration compares to erbium and germanium. A similar trend shows

in Figure 4.12 for 3 and 9 droplets in multiple cycles. An increasing in counts of erbium ion is detected as the position moved towards to ring. Higher counts implied the higher erbium ion concentration as equal to that in one cycle. However, the graph shows a dramatically increase as compared to that one cycle. This implies the non-uniformity in selective area doping for multiple cycle is due to the high erbium ion distribution in ring position.

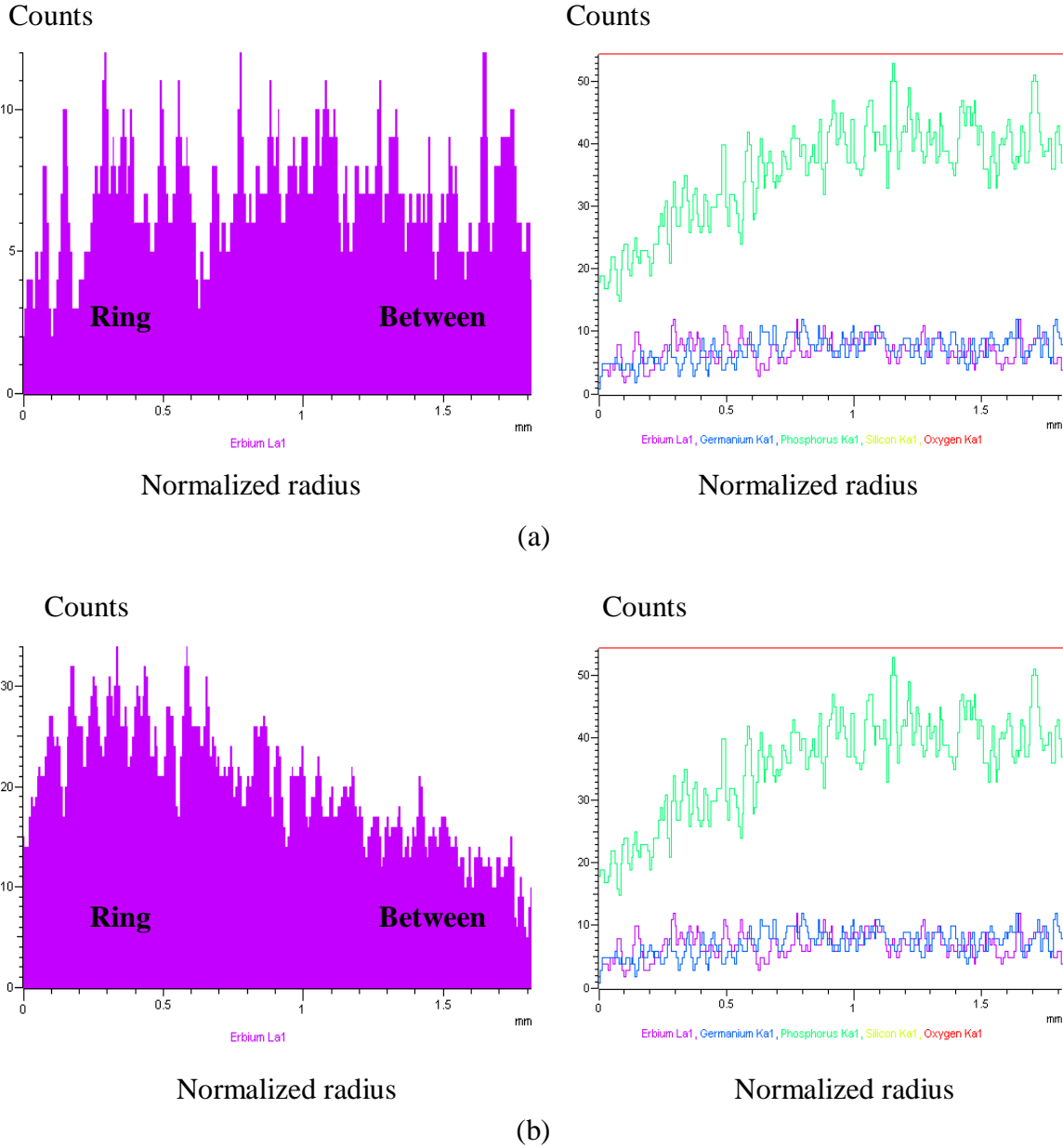
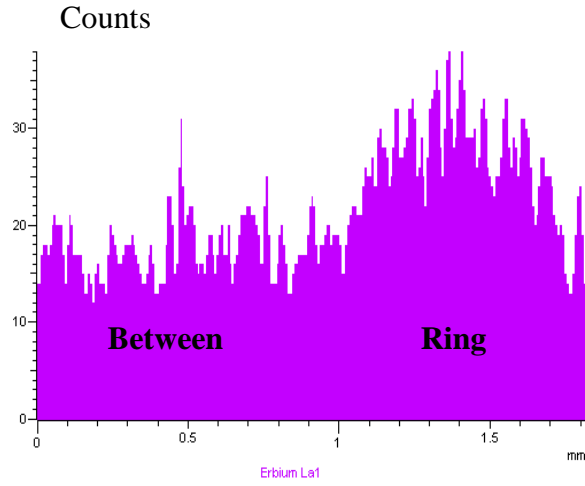
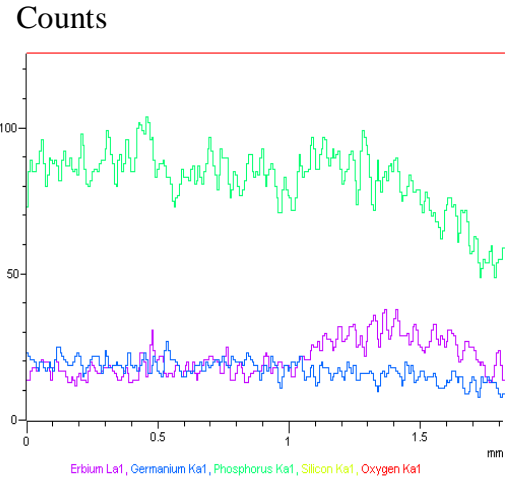


Figure 4.11. EDX profile across circle in selective area doping in 0.1M erbium chloride by using syringe (one cycle) (a) 3 droplets (b) 9 droplets



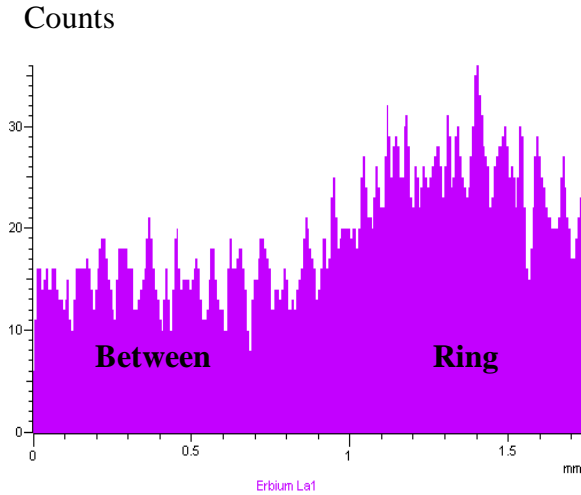


Normalized radius

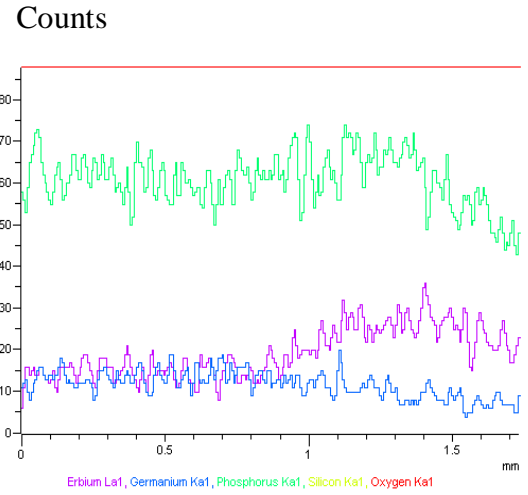


Normalized radius

(a)



Normalized radius



Normalized radius

(b)

Erbium Germanium Phosphorus Oxygen

Figure 4.12. EDX profile across circle in selective area doping in 0.1M erbium chloride by using syringe (multiple cycles) (a) 3 droplets (b) 9 droplets

#### 4.5 Selective area by pipette & hotplate

There are two main problems face during using syringe in selective area doping. They are controlling the volume of droplets and over flow of diffusion into other doping area. Furthermore, the volume of every droplet can not be maintained. This leads too many ring appear in selective area doping as showed in section above. This problem can be overcome by using a pipette. In our work, the pipette used could vary in volume range of 0.1  $\mu\text{L}$  to 2.5  $\mu\text{L}$ . The volume for each droplet could control as well when using pipette compared to syringe. The effect of many rings appearance in selective area doping will not happened. Over flow of solution to other doping areas is due to the continuously dripping in one selective area doping. Multiple cycles could overcome the solution overflow issue. Controlling spread of doping area can be done by drying method in multiple cycles. A method to use pipette and hotplate in controlling spread of doping area is introduced in this section illustrate in Figure 4.13. Temperature plays a role to control the spread of doping area or diameter circle. As temperature increases, the solution drip by pipette will be dried up in shorter time leads to strictly reduce the diffusion of solution. The spread of doping area reduces as the diffusion of solution strictly limits. In addition, the volume of droplets could be control. As the volume of droplets reduce in results the spread of doping area also limits. The spread of doping area can be affected by droplets volume and substrate temperature. The minimize spread of doping area is preferred apply in waveguide. The hotplate was calibrated. An off-set graph was used as reference to show the comparison hotplate temperature to substrate temperature.

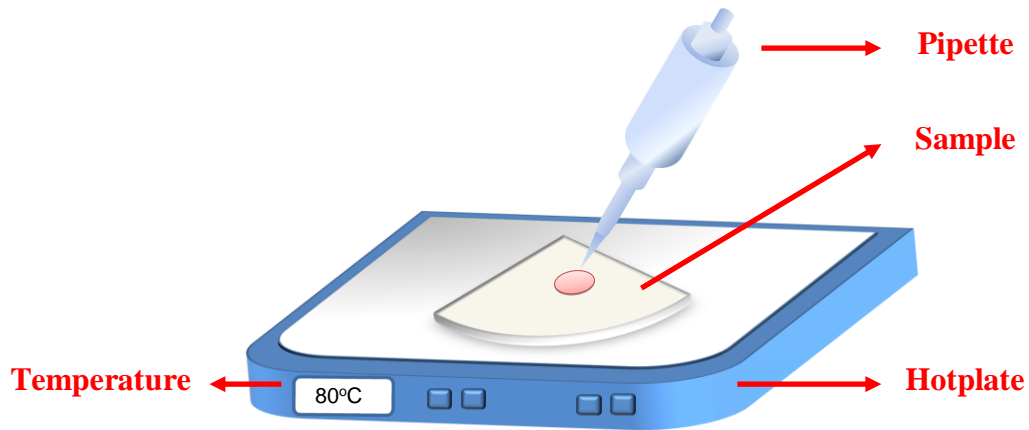
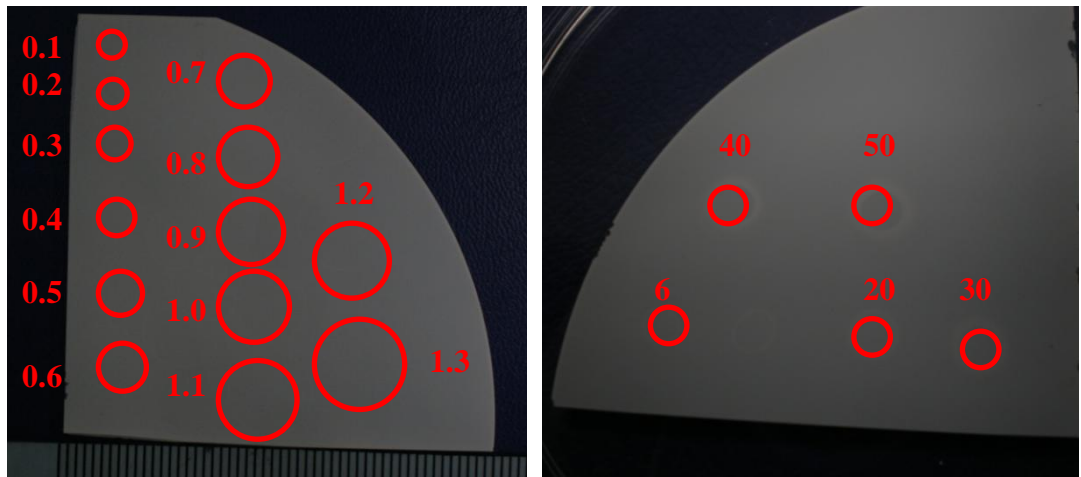


Figure 4.13 Schematic of selective area doping by using pipette and hotplate to adjust the temperature.

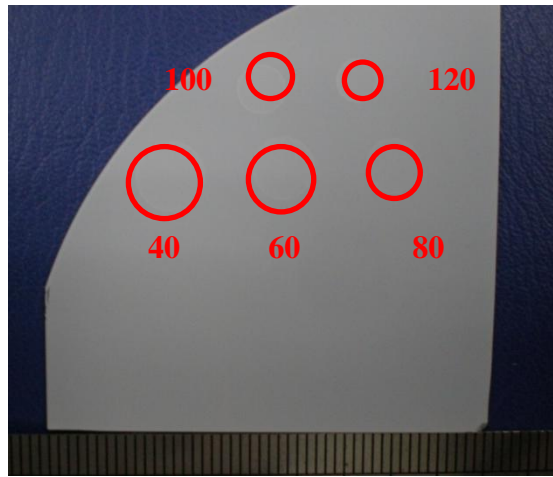
#### 4.5.1 Diameter of selective doping area

Similar to the syringe method, a variation of spread diameter was investigated. The volume of droplets, temperature and multiple cycles were used to vary the diameter of circle. Figure 4.14 shows the samples in change with volume of droplets, multiple cycles and temperature effect to diameter of circle. One droplet was dripped into silica soot layer for Figure 4.14 (a) and (c). From the picture, the spread diameter of circles is smaller than that when using syringe due to reduction in volume of droplets. For picture 4.15 (a), volume of droplets is varied from  $0.1 \mu\text{L}$  to  $1.3 \mu\text{L}$  by using pipette. As shows in picture, the diameter of circle increases as the volume increases.  $0.1 \mu\text{L}$  is the smallest spread diameter of circle in selective area doping and is suit able for waveguide. As a result,  $0.1 \mu\text{L}$  is used in multiple cycles and  $0.02\text{M}$  erbium chloride is used to drip by using pipette. The diameter of circles seen is not affected much as the number of droplets increases like the result in multiple cycles by using syringe. Ring appearance becomes obvious as the number of droplets increases. The spread size of circle decreases as temperature increases when the substrate is heated by the hotplate. These can be proven in the results of diameter measurement in below.



(a)

(b)



(c)

Figure 4.14. Pictures of samples in selective area doping by using pipette (a) volume of droplets varied from 0.1  $\mu$  to 1.3  $\mu$ L drip in 0.02M erbium chloride (b) multiple cycles with change in number of droplets drip in 0.02M erbium chloride (c) hotplate and 0.5  $\mu$ L volume of droplets drip in 0.1M erbium chloride

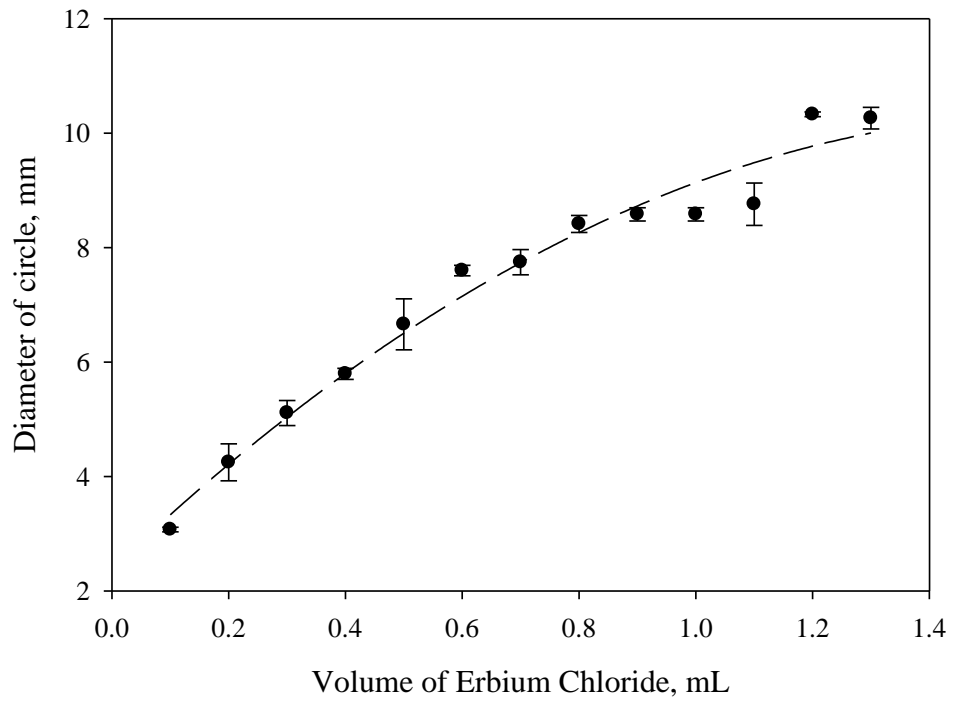


Figure 4.15. Graph showing the diameter of circle, mm varied with volume of erbium chloride,  $\mu\text{L}$ .

Table 4.3. Diameter of circle varied with volume of droplets

Volume of droplets, $\mu\text{L}$	Diameter of circle, mm $\pm 0.005$
0.1	3.072
0.2	4.247
0.3	5.109
0.4	5.793
0.5	6.659
0.6	7.598
0.7	7.744
0.8	8.413
0.9	8.581
1.0	8.755
1.1	10.328
1.2	10.262
1.3	11.288

Graph in Figure 4.15 shows that diameter of circle measured by analysis software, Images J. As seen in the graph, the diameter of circle increases as the volume of erbium chloride solution increases. It gradually increases from 3.072 mm to 11.288 mm similar to that the shown in Figure 4.14 (a). Area of diffusion spread is wider as the volume of solution increases, leading to the increases of the circle diameter. The measured figure showed in Table 4.4. As a result, 0.1  $\mu\text{L}$  in spread of circle diameter i.e 3.072 mm shows the smallest spread area serve as a suitable to dope in waveguide. The increasing of diameter is not constant as add 0.1  $\mu\text{L}$  for every droplet. The research attention moves to multiple cycles by using pipette. A gradually increasing form in graph shows in Figure 4.16. The diameter of circle increases by  $\sim 24.88\%$  from 3.239 mm to 4.045 mm as 44 droplets was added. The diffusion occurs as the droplets were added into silica soot layer. Molecular force in silica soot layer will put forwards the spread of circle as the droplets add into silica soot layer. A gradual increasing trend is shown in the ring width ranging from 0.315 mm to 0.977 mm. A peak shown in the graph is due to the largest ring width when 30 droplets were added. The ring appearance shows the erbium ion accumulated. This can be proved by EDX results.

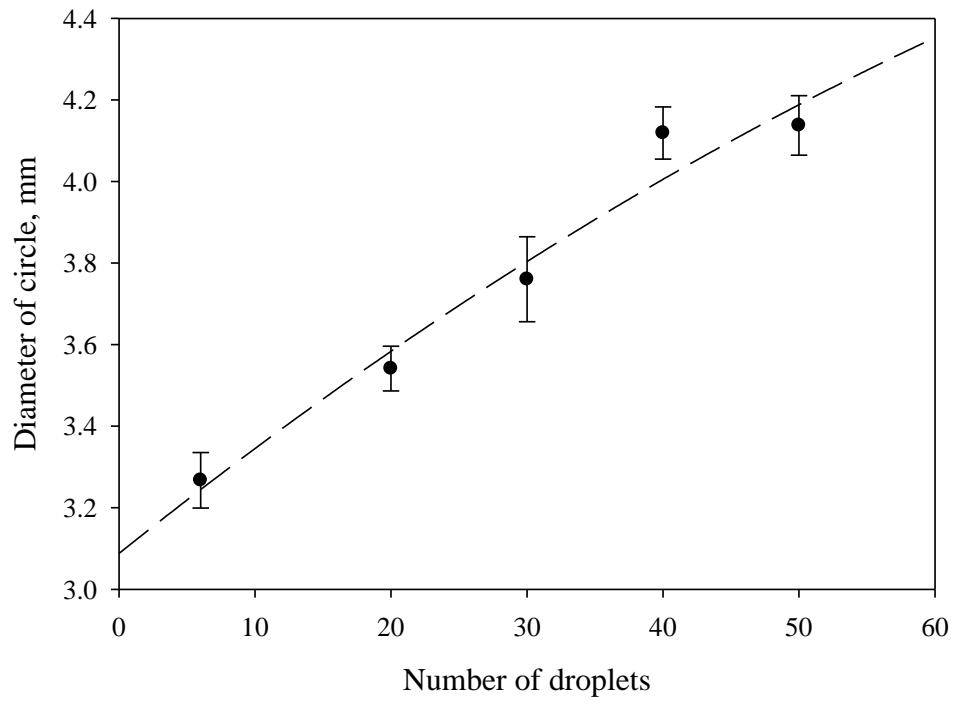


Figure 4.16. Graph showing the diameter of circle, mm varied with number of droplets in multiple cycles

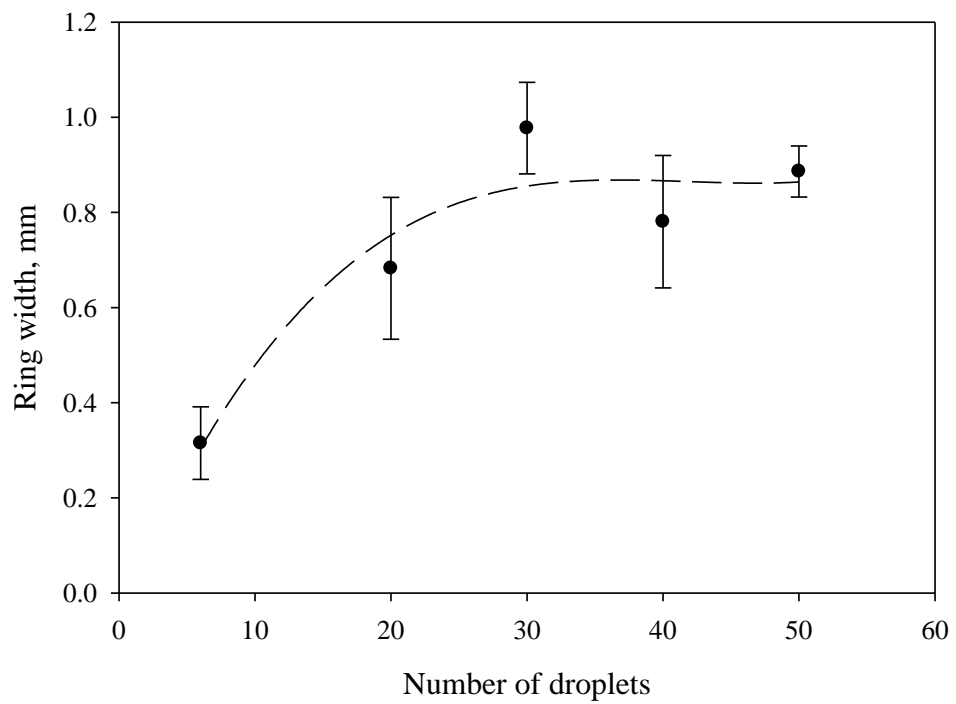


Figure 4.17. Graph showing ring width, mm varied with number of droplets in multiple cycles

Table 4.4. Diameter of circle and ring width in multiple cycles by using pipette

Number of droplets	Diameter of circle, mm $\pm 0.005$	Ring width, mm $\pm 0.005$
6	3.239	0.315
20	3.576	0.683
30	3.727	0.977
40	4.045	0.781
50	4.045	0.886

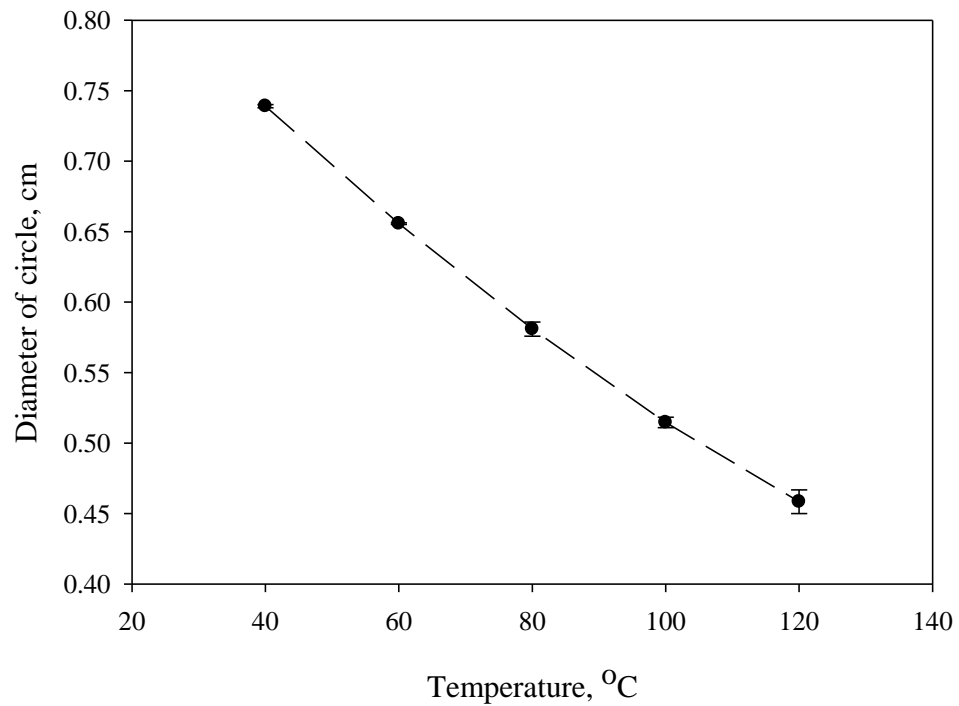


Figure 4.18. Graph showing diameter of circle, mm varied with temperature, °C by using hotplate and pipette.

Table 4.5. Diameter of circle varied with temperature

Temperature, °C	Diameter of circle, mm $\pm 0.005$	Reduction of circle, mm $\pm 0.005$
40	0.739	-
60	0.656	0.083
80	0.582	0.074
100	0.516	0.066
120	0.458	0.058



Temperature plays a role in reducing the spread diameter. As shown in Figure 4.18, there is a decreasing trend in diameter of circle as the temperature is increased. The diameter of circle decreases ~ 38% from 0.739 mm to 0.458 mm as the temperature varies 40°C to 120°C. As mentioned above, the erbium chloride solution dries up as substrate is heated. Spread of circle diameter or diffusion is limited as the temperature increases. As a result, the diameter of circle reduces. However, there is a limitation to reduce circle diameter in change with temperature. Table 4.4 shows that the decreasing trend in diameter of circle as temperature increases. We also need to concern about the controlling in temperature. The high temperature will cause evaporation of solution. This will be effect to erbium ion incorporate in silica soot layer.

#### **4.5.2 Erbium ion concentration Vs number of droplets**

EDX was used to measure the composition of layers fabricated using multiple cycles. Similar to the measured method used in the syringe case, three positions were taken to measure the erbium ion concentration. They were center, between and ring. We also use the same measurement method to determine composition in multiple cycles by using pipette. The results show that there is no erbium ion detected in positions of center and between. For the ring position, an increasing trend shows in Figure 4.19 as the number of droplets increases. High erbium ion concentration incorporated in ring position of silica soot layer even for a low strength 0.02M erbium chloride solution was used. The high erbium ion concentration was achieved by adding 40 to 50 droplets into silica soot layer. This is proven that accumulated erbium ion in the ring position as same as multiple cycles in syringe. For multiple cycles, it seems similar incorporation erbium ion concentration level in 3 droplets by using syringe and 40 and 50 droplets by using pipette.

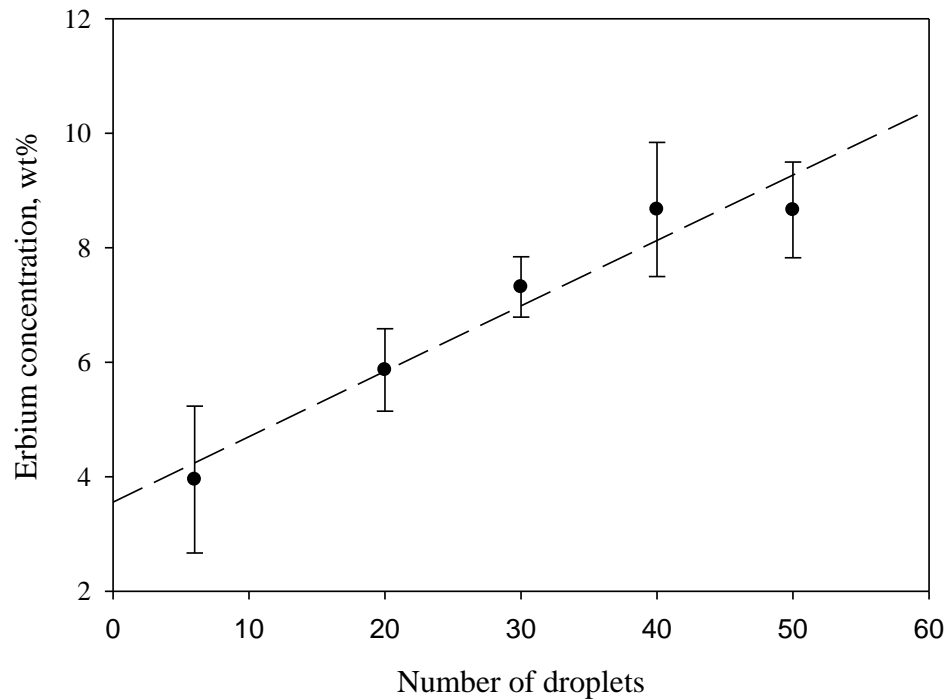
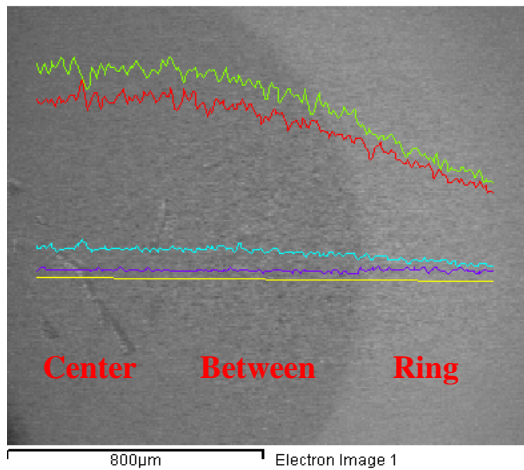


Figure 4.19. Graph showing erbium ion concentration, wt% with change in number of droplets in ring position dope with 0.02M erbium chloride by using pipette (multiple cycles)

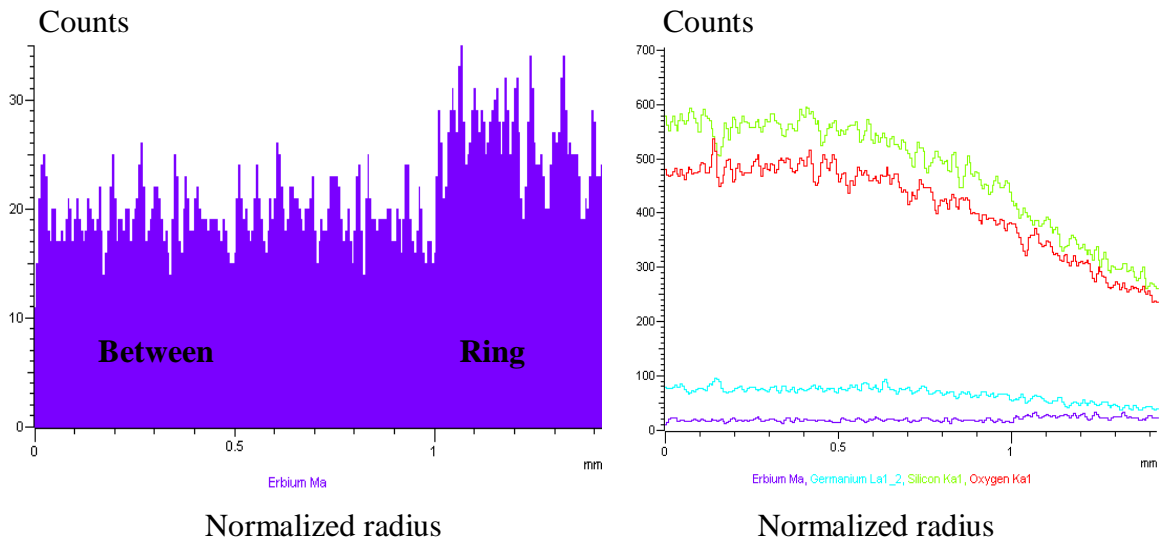
### 4.5.3 Distribution of erbium ion concentration

The similar trend in distribution of erbium ion concentration with the results in syringe shows in Figure 4.21. High erbium ion counts are collected by detector in ring position compares to between and center positions. High erbium ion accumulates in ring position leads to high concentration in ring positions. The silicon and oxygen composition decreases from center towards ring position. Figure 4.20 shows the position of circle as line scan was taken in distance 1.6 mm. Desired distribution of erbium ion concentration is constant and uniformity as moved center towards to ring position. This can be achieving by continuously dripping in selective area. However, spread of diameter shall be control as well as.



Erbium Germanium Silicon Oxygen

Figure 4.20. Images showing the position of circle during line scan was taken by using EDX.



Erbium Germanium Silicon Oxygen

Figure 4.21. EDX profile across circle in selective area doping in 0.1M erbium chloride by using pipette for 50 droplets. (multiple cycles)

#### 4.6 Summary

In this chapter, selective area doping in silica soot layer had been described. An introduction to explain why selective area doping should be develops in integrated optic. Selective area doping had been used in semiconductor compound as purpose for different

substrate material. A review described the similar selective area doping by using different doping method that applied in semiconductor compound in integrated optic or electronic technology. The development of research moved to solution doping serve as easier and low cost method to incorporate rare-earth ion into silica layer. They are two dripping equipments used in this experiment i.e. syringe and pipette with hotplate. Experimental method had been explained and the variations of diameter, erbium ion concentration and distribution were investigated. Different kind of parameters used to vary the variations such as dripping method i.e. one cycle and multiple cycle, number of droplets and dripping equipment.

**Reference:**

- [1] F. Z. Tang, P. McNamara, G. W. Barton, and S. P. Ringer, "Nanoscale characterization of silica soots and aluminium solution doping in optical fibre fabrication," *Journal of Non-Crystalline Solids*, vol 352, pp.3799, 2006.
- [2] A. Dhar, M. C. Paul, M. Pal, S. K. Bhadra, H. S. Maiti, and R. Sen, "An improved method of controlling rare earth incorporation in optical fiber," *Optics Communications*, vol 277, pp.329, 2007.
- [3] F. Z. Tang, P. McNamara, G. W. Barton, and S. P. Ringer, "Multiple solution-doping in optical fibre fabrication I - Aluminium doping," *Journal of Non-Crystalline Solids*, vol 354, pp.927, 2008.
- [4] F. Z. Tang, P. McNamara, G. W. Barton, and S. P. Ringer, "Multiple solution-doping in optical fibre fabrication II - Rare-earth and aluminium co-doping," *Journal of Non-Crystalline Solids*, vol 354, pp.1582, 2008.
- [5] D. L. Miller, T. Oaks, and Calif, (Rockwell International Corporation, EI Segundo, Calif, 1984).
- [6] J. R. G. Andrew Shaw, James F. Shackelford, Enrique J. Lavernia, Michael T. Powers, *Materials Processing Handbook* (CRC Press, 2007), p. 840.

## Chapter 5

### 5.1 Summary

Doping of silica glass layers with erbium by using solution doping had been demonstrated during the work described in this thesis. An introduction to silica-on-silica technology was given. Silica is chosen due to low cost in fabrication, compatible with silica fiber results reducing splicing problems. In addition, good adhesion between silica and silicon wafer leads to silica being the preferred choice for integrated optics. A more detail about glass structure and how dopants effect to silica layer had been explained. Erbium is the main choice of rare-earth material in our thesis. The principle of amplifier in erbium and the gain limiting effect in amplifier had been explained. The fabrication of erbium doped silica glass layer involves two steps. It combines the deposition of silica soot layer by flame hydrolysis deposition (FHD) following the solution doping. Two types of solution doping technique were used in this thesis. Non-selective area doping involves the whole area of samples while selective area doping were used to minimize the spread of doping area. Erbium chloride ( $\text{ErCl}_3 \cdot 6\text{H}_2\text{O}$ ) aqueous solution was used to incorporate erbium ion into silica soot layer. The experimental method had been explained. In non-selective area doping, the variation of erbium ion concentration, thickness and number of pores per square area were investigated in different pre-sintering temperature of silica soot layer. Besides, the parameter such as strength of solution and dipping period were used to vary the erbium ion concentration incorporated. Selective area doping had been explained in experimental method. An effort in minimizing and controlling the spread of doping area, selective area doping was used to incorporate erbium ion. A similar selective area doping had been described which used different doping method. This review is applied in semiconductor compound for integrated optic or electronic technology. There are two dripping equipments used in

this experiment i.e. syringe and pipette with hotplate. Experimental method had been explained and the variations of diameter, erbium ion concentration and distribution were investigated. Different kinds of parameters used to vary the variations such as dripping method i.e. one cycle and multiple cycle, number of droplets and dripping equipment.

## 5.2 Conclusion

Monolithic integrated of glass-based optical devices has been demonstrated by using flame hydrolysis deposition (FHD) to deposit silica soot layer following by solution doping. Solution doping is used to incorporate erbium ion into silica soot layer. The key conclusions from this study are as follow:

- The morphology and structure of silica soot layer varied as pre-sintering temperature changed. The agglomeration in size of particles becomes larger and skeleton of glass structure is stronger as pre-sintering temperature increased. The pore size also increased. After solution doping, the structure of silica soot layer become fluffy. White particles appear in silica soot layer. The identified of white particles still run in progress. However, the skeleton of glass layer is compacted and stronger in pre-sintering 950°C before and after solution doping.
- In calculation number of pores per square area in silica soot layer, 850°C showed the optimum pre-sintering temperature due to the highest number of pores per square area among 750°C to 950°C. The thickness of soot layer decreased as pre-sintering temperature increased and also after solution doping.
- The erbium ion concentration incorporated did not show a significant trend as varied pre-sintering temperature. The pre-sintering temperature did not affect to erbium ion concentration.

- For non-selective area doping, the erbium ion concentration incorporated increased with the strength of solution. The refractive index of glass silica give rise as the strength of solution increased. The dipping period manage a saturation point in 20 minutes for erbium ion incorporation in silica soot layer. The erbium ion concentration graph showed a fluctuation line after 20 minutes indicated a saturation point.
- For selective area doping, the diameter of circle and ring width increased with number of droplets for one and multiple cycle by using syringe and pipette. The increasing in diameter of circle was not effect much in multiple cycles compared to one cycle. The diameter of circle increased with volume of droplets but decreased as temperature increased.
- High erbium ion concentration achieved in ring position of circle for multiple cycles by using syringe and pipette. Non-uniformity of doping occurred in multiple cycles. For one cycle, the distribution of erbium ion concentration is quite uniformity.
- The erbium ion concentration incorporated increased as number of droplets increased and move from center towards to ring position.

### **5.3 Future work**

The silica glass layer is formed and doped with erbium ion. Others variations can be done to vary the erbium ion concentration such as soaking times. As the number of soaking time increase, the erbium ion concentration increases [1]. The samples will dip into erbium chloride aqueous solution and following by the drying and dehydration method. The samples will dip again into aqueous solution for second times and further. The distribution of erbium ion measured by EDX indicates the uniformity of doping. The porosity of silica soot layer can be calculated by images J. A pore area fraction, defined by the ratio of total pore area to area of deposit as increased in temperature. The

porosity can define the structure of silica soot layer in direct effect to erbium ion incorporation. For selective area doping, the strength of solution can be vary as temperature increase. The spread of doping area will be varied by change the strength of solution. Co-doping with other rare-earth ion is known to significantly suppress such clustering. Co-doping method had been tested by my lab partner such as ytterbium. As the optimum condition achieved in glass layer, optical properties such as photoluminescence, fluorescence life time and optical loss can be tested [2-5]. An erbium doped waveguide amplifier on silica-on silicon can be established as the optimum condition achieved.

## References

- [1] F. Z. Tang, P. McNamara, G. W. Barton, and S. P. Ringer, "Multiple solution-doping in optical fibre fabrication II - Rare-earth and aluminium co-doping," *Journal of Non-Crystalline Solids*, vol **354**, pp.1582, 2008.
- [2] J.R.Bonar, M.V.D.Vermelho, P.V.S.Marques, A.J.McLaughlin, and J.S.Aitchison, "Fluorescence lifetime measurement of aerosol doped erbium in phosphosilicate planar waveguides," *Optics Communications*, vol **149**, pp.27, 1998.
- [3] A. Najar, J. Charrier, H. Ajlani, N. Lorrain, H. Elhouichet, M. Oueslati, and L. Haji, "Optical properties of erbium-doped porous silicon waveguides," *Journal of Luminescence*, vol **121**, pp.245, 2006.
- [4] J. R. Bonar, J. A. Bebbington, J. S. Aitchison, G. D. Maxwell, and B. J. Ainslie, "Low threshold Nd-doped silica planar waveguide laser," *Electronics Letters*, vol **30**, pp.229, 1994.
- [5] D. Shin, "Photoluminescence of erbium-doped silica based waveguide film via flame hydrolysis deposition and aerosol doping," *Journal of Ceramic Processing Research*, vol **7**, pp.379, 2006.



## **List of Publications**

S.T.Kow, Y.Yap, C.H. Pua, W.Y.Chong, A.W.P.Law, F.R.Mahamd Adikan, A.S.M.A.Haseeb, H.Ahmad, "Selective area rare-earth doping of planar glass samples for monolithic integration of optically passive and active waveguides", Optik, Article In Press, 2009.